

## Seasonal variations of C<sub>2</sub>–C<sub>4</sub> nonmethane hydrocarbons and C<sub>1</sub>–C<sub>4</sub> alkyl nitrates at the Summit research station in Greenland

Aaron L. Swanson and Nicola J. Blake

Department of Chemistry, University of California at Irvine, Irvine, California, USA

Elliot Atlas and Frank Flocke

Atmospheric Chemistry Division, National Center for Atmospheric Research, Boulder, Colorado, USA

Donald R. Blake and F. Sherwood Rowland

Department of Chemistry, University of California at Irvine, Irvine, California, USA

Received 31 October 2001; revised 7 August 2002; accepted 1 September 2002; published 28 January 2003.

[1] We report measurements of light (C<sub>2</sub>–C<sub>4</sub>) nonmethane hydrocarbons (NMHCs) and C<sub>1</sub>–C<sub>4</sub> alkyl nitrates made at Summit, Greenland, over a full annual cycle (June 1997–1998). The remoteness of the Summit camp from industrial source regions resulted in trends of these trace gases that showed a clear seasonal variation with low variability. Variability (calculated as the percentage 1-sigma deviation of a running 10-point mean) averaged 7–9% for ethane over the entire study. The shorter-lived species (ethyne, propane, and the butanes) exhibited variability from 12–20% in winter to 20–100% in summer. The best fit curve to the annual cycle of ethane is a sinusoidal oscillation, but each of the shorter-lived NMHCs exhibited flat periods of low concentrations during the summer months. The C<sub>2</sub>–C<sub>4</sub> NMHCs peaked between 8 and 24 February, with the longer-lived NMHCs maximizing latest. These data were broadly consistent with literature values, confirming that high-latitude Northern Hemisphere (NH) emissions are similar year to year. Employing their linear fall accumulation rates, we calculated average NMHC ratios versus ethane of 0.59(±0.10):0.33(±0.05):0.26(±0.08):0.14(±0.04) for propane, ethyne, *n*-butane, and *i*-butane, respectively. We suggest that these ratios represent useful quantities with which to compare averaged mid- and high-latitude NH emission ratios. We also report the first year-round observations of the seasonal cycle of light C<sub>1</sub>–C<sub>4</sub> alkyl nitrates. Similar to the NMHCs, the seasonal trend of these gases shows primary dependence on transport to Summit during winter, and photochemical removal during summer. Unlike their parent NMHCs, alkyl nitrate concentrations did not asymptote to low levels during summer and they exhibited winter maxima later with decreasing photochemical lifetime. **INDEX TERMS:** 0322 Atmospheric Composition and Structure: Constituent sources and sinks; 0365 Atmospheric Composition and Structure: Troposphere—composition and chemistry; 0368 Atmospheric Composition and Structure: Troposphere—constituent transport and chemistry; **KEYWORDS:** NMHC, ethane, organic nitrates, emission ratios

**Citation:** Swanson, A. L., N. J. Blake, E. Atlas, F. Flocke, D. R. Blake, and F. S. Rowland, Seasonal variations of C<sub>2</sub>–C<sub>4</sub> nonmethane hydrocarbons and C<sub>1</sub>–C<sub>4</sub> alkyl nitrates at the Summit research station in Greenland, *J. Geophys. Res.*, 108(D2), 4065, doi:10.1029/2001JD001445, 2003.

### 1. Introduction

[2] The seasonality of light nonmethane hydrocarbons (NMHCs) has been well documented for the Northern Hemisphere (NH) [Hov *et al.*, 1984; Blake and Rowland, 1986; Rudolph, 1995] and at specific NH sites including a mountain site in Scandinavia [Laurila and Hakola, 1996], rural New England [Goldstein *et al.*, 1995a], the Mauna Loa Observatory [Greenberg *et al.*, 1996], the North Atlantic Ocean [Penkett *et al.*, 1993], a remote boreal site in Canada [Jobson *et al.*, 1994a], rural locations across Canada [Bot-

tenheim and Shepherd, 1995], coastal Sweden [Lindskog and Moldanova, 1994], and rural Japan [Sharma *et al.*, 2000], among others. Seasonal variations in NMHC concentrations are influenced by: (1) photochemical removal (primarily by the hydroxyl (OH) radical), (2) NMHC source strengths, (3) dilution due to atmospheric mixing of air parcels [Roberts *et al.*, 1984, 1985; Rudolph and Johnen, 1990; McKeen *et al.*, 1996], and (4) transport dynamics from source regions to the sampling site [Barrie, 1986; Cassano *et al.*, 2001; Klonecki *et al.*, 2003]. Seasonal changes in anthropogenic NMHC source strengths are thought to be small [Jobson *et al.*, 1994b; Poisson *et al.*, 2000] because they are largely driven by constant urban fossil fuel combustion and leakage from oil and natural gas production

[Friedrich and Obermeier, 1999]. For the light NMHCs of interest (ethane, propane, ethyne, *iso*- and *n*-butane), urban or industrial sources will have higher emissions from evaporation during summer, particularly for the butanes. The C<sub>2</sub>–C<sub>4</sub> NMHCs are not emitted in significant quantities by natural (biogenic) sources [Guenther *et al.*, 2000], but biomass burning (which is seasonally dependent) is a large source for C<sub>2</sub>–C<sub>3</sub> NMHCs [Rudolph, 1995; Gupta *et al.*, 1998]. By contrast, transport and photochemical removal are strongly seasonal. Transport to high latitudes is dependent on strong meridional flow and weak convection from continental areas during winter, while the opposite conditions exist during summer [Kahl *et al.*, 1997, 1999; Steffen and Box, 2001; Klonecki *et al.*, 2003]. Photochemical removal is also seasonally dependent with roughly a 100-fold increase in OH concentration from winter to summer at high latitudes [Spivakovsky *et al.*, 2000]. It is thought that photochemical removal is the dominant factor influencing seasonal changes in NMHC concentrations [Jobson *et al.*, 1994a; Goldstein *et al.*, 1995a; Rudolph, 1995]. This is supported by the strong seasonal variations observed at midlatitude sites that are within primary source regions themselves (which presumably should not be dependent on transport) [Hagerman *et al.*, 1997; Sharma *et al.*, 2000].

[3] However, source distributions of C<sub>2</sub>–C<sub>4</sub> NMHCs are not well constrained and the amount of each NMHC released from source areas such as urban centers [Parrish *et al.*, 1992], remote oil and natural gas production [Blake *et al.*, 1992], or biomass burning [Andreae and Merlet, 2001] regions is highly variable. To better constrain emission estimates, a large effort has been made by the international community to create emission inventories in programs such as the Emission Database for Global Atmospheric Research (EDGAR) developed within the Global Emission Inventory Activity (GEIA), a component of the International Global Atmospheric Chemistry Program (IGAC) [Olivier *et al.*, 1996, 1999]. EDGAR is a database of global inventories of direct and indirect greenhouse gas emissions from anthropogenic sources on a per country basis as well as on 1° × 1° grid [Olivier *et al.*, 1996, 1999]. These inventories are important inputs for global and regional chemistry models that try to predict or forecast tropospheric chemistry. The light NMHCs are important trace gases for global chemistry models as they are the longest-lived NMHCs and they represent a dominant fraction of reactive organic carbon species in remote regions and at high latitudes. Species such as ethane also provide a source of peroxyacetyl nitrate (PAN) to the remote atmosphere [Atkinson, 2000].

[4] The NMHCs are also precursors to ozone (O<sub>3</sub>) in the troposphere [Haggen-Smit, 1952]. Large efforts have been made to model ozone distributions on the municipal, regional, and global levels, as O<sub>3</sub> is an important greenhouse gas and oxidant in the lower atmosphere [Schere and Hidy, 2000]. The balance between the formation and destruction of ozone in both urban and remote regions of the troposphere is determined by the ratio of volatile organic hydrocarbons (VOCs) to NO<sub>x</sub> (NO + NO<sub>2</sub>) [e.g., Ridley *et al.*, 1987]. A feature of tropospheric ozone that is thought to have significant contributions from both chemical and dynamic origins is the widely observed springtime maximum at NH midlatitudes. The winter buildup of NMHCs, followed by rapid springtime photochemical destruction, is

suggested to play a significant role in this ozone maximum [Penkett and Brice, 1986; Penkett *et al.*, 1993; Yienger *et al.*, 1999]. The Tropospheric Ozone Production about the Spring Equinox project (TOPSE) recently studied springtime ozone production, highlighting the fact that knowledge of the seasonal abundance of NMHCs and NO<sub>x</sub> in the remote atmosphere is crucial to our understanding of their influence on seasonal ozone levels [Blake *et al.*, 2003a].

[5] Because the lifetime of NO<sub>x</sub> is very short (hours to days depending on atmospheric conditions) [Finlayson-Pitts and Pitts, 2000], its background mixing ratio in the remote atmosphere, especially in the Arctic, is very low, often below detection [Honrath and Jaffe, 1992]. Therefore it is important to measure species that can generate NO<sub>x</sub>, i.e., NO<sub>x</sub> reservoir species. The large group of NO<sub>x</sub> reservoir species collectively known as NO<sub>y</sub> include NO<sub>x</sub> + HNO<sub>3</sub> + HONO + organic nitrates + others. PAN and the alkyl nitrates (RONO<sub>2</sub>) are thought to be the primary organic nitrate components.

[6] The dominant atmospheric formation pathways for alkyl nitrates are natural (oceanic) and anthropogenic hydrocarbon (HC)-NO<sub>x</sub> photochemistry. Alkyl nitrates lighter than C<sub>4</sub> are removed principally not only by photolysis, but also by reaction with OH [Clemmishaw *et al.*, 1997]. The rate of photolysis, as well as the rate of reaction with OH, increases with increasing HC chain length so that average atmospheric lifetimes decrease rapidly with increasing carbon number [Clemmishaw *et al.*, 1997].

[7] Formation of alkyl nitrates through HC-NO<sub>x</sub> photochemistry gives an increasing yield of the alkyl nitrate with increasing HC chain length [Atkinson *et al.*, 1982; Roberts, 1990; Arey *et al.*, 2001]. As a consequence, polluted continental regions produce large quantities of C<sub>4</sub> and heavier alkyl nitrates, although due to diminishing atmospheric lifetimes with longer chain length, polluted air masses tend to be dominated by C<sub>3</sub>–C<sub>5</sub> alkyl nitrates [Bertman *et al.*, 1995; Flocke *et al.*, 1998; Blake *et al.*, 2003a]. While alkyl nitrate emissions from the ocean are dominated by C<sub>1</sub>–C<sub>2</sub> RONO<sub>2</sub>, with highest marine boundary layer (MBL) concentrations over the equatorial Pacific Ocean [Atlas *et al.*, 1997; Blake *et al.*, 2003b] and the Southern Ocean [Blake *et al.*, 1999].

[8] Here we present results from a seasonal study of light NMHCs at Summit, Greenland, as well as the first measurements of the full seasonal cycle of light alkyl nitrates at a remote Arctic location. A winter-spring peak was recorded for the C<sub>3</sub>–C<sub>6</sub> alkyl nitrates during the Polar Sunrise Experiment (PSE) at Alert Canada in 1992 [Muthuramu *et al.*, 1994], similar to the total alkyl nitrate winter-spring trend recorded during PSE 1988 [Bottenheim *et al.*, 1993]. In addition, the concentrations of C<sub>2</sub>–C<sub>6</sub> alkyl nitrates decreased during spring-time in the interior of Alaska in 1993 [Beine *et al.*, 1996], but we do not know of any other partial seasonal studies. The only other full alkyl nitrate seasonal study was recorded during four seasonal intensives at the Mauna Loa Observatory [Atlas and Ridley, 1996].

## 2. Experimental Procedure

[9] Lying at 38.48°W longitude, 72.57°N latitude atop the Greenland ice cap at 3200 m, Summit is far removed from anthropogenic source regions. The only known C<sub>2</sub>–C<sub>4</sub>

alkane and ethyne sources within 400 km of Summit are emissions from the research camp itself, which is positioned in a 60° sector 300 m to the north of the sampling site (where winds tend to be Southerly). Occasional resupply flights, snow mobile usage, and heavy machinery to move snow offer potential local contamination. Normal usage of these mobile sources are kept in the N sector, but due to the close proximity of the camp, contamination periodically impacts the clean air sampling site.

[10] Whole air samples were collected in evacuated electropolished stainless steel canisters from 14 June 1997 until 20 June 1998. The canisters were filled to a pressure of 40 psi using a viton diaphragm pump connected to a stainless steel inlet line positioned on a sampling tower at 1 m above the snow surface from 14 June 1997 to 8 April 1998. After 8 April until the end of the project in June, samples were collected without the use of a pump by simply opening the evacuated canister and allowing it to fill to ambient pressure. Sampling was conducted roughly every 2 days at midday over the study period. During the first three fourths of the project, when samples were pressurized, the sampling was performed 300 m south of the camp in a clean air sector. Sampling was avoided when wind was blowing from the northern direction of the camp generators or living quarters or when the winds were stagnant ( $<1 \text{ m s}^{-1}$ ). During the last one fourth of the project, when samples were collected to ambient pressure, the samples were collected at random locations around the camp upwind of camp emissions. Once filled, the canisters were normally returned to our laboratory at the University of California, Irvine (UCI) at regular monthly intervals for analysis, except over the four winter months of complete solar darkness when resupply flights were not possible and samples had to remain at camp.

[11] The analytical technique employed has been thoroughly described by *Chen* [1996], *Sive* [1998], and *Colman et al.* [2001]. Briefly, a 1519  $\text{cm}^3$  aliquot of each air sample was cryofocused onto a stainless steel trap packed with glass beads, then warmed to  $\sim 80^\circ\text{C}$  and injected into a helium gas stream and split to five gas chromatographs (GCs). The NMHCs were separated by a J & W Scientific silica PLOT column (30 m, 0.53 mm) connected to a flame ionization detector (FID). The detection limit of each NMHC was 1 pptv. The alkyl nitrates were separated by a Restek 1701 capillary column (60 m, 0.25 mm, 1  $\mu\text{m}$ ) connected to an electron capture detector. The detection limit for the alkyl nitrates was 0.1 pptv. All NMHCs were calibrated against whole air working standards, which have been calibrated against NIST and Scotty standards [*Sive*, 1998]. The precision of our  $\text{C}_2\text{--C}_4$  NMHC analysis is  $\pm 3\%$  when compared to NIST standards during the Nonmethane Hydrocarbon Intercomparison Experiment (NOMHICE) [*Sive*, 1998]. Alkyl nitrates were calibrated against whole air working standards, which had been previously calibrated to an accuracy of better than 2% against a synthetic standard provided by Elliot Atlas and Frank Flocke of the National Center for Atmospheric Research. The alkyl nitrate precision is better than  $\pm 5\%$  for all compounds. Carbon monoxide (CO) was also measured in the canister samples employing the methods described by *Hurst* [1990] and *Lopez-Palma* [2002], using a packed column GC separation of CO followed by reduction to methane on a nickel catalyst

and detection by FID. The absolute accuracy of the CO measurements calibrated against NIST standards was  $\pm 7\%$ , with a DL of 5 ppbv [*Lopez-Palma*, 2002].

### 3. Results

#### 3.1. NMHCs

[12] The  $\text{C}_2\text{--C}_4$  NMHCs, ethane ( $\text{C}_2\text{H}_6$ ), propane ( $\text{C}_3\text{H}_8$ ), ethyne ( $\text{C}_2\text{H}_2$ ), *n*-butane ( $n\text{-C}_4\text{H}_{10}$ ), and *i*-butane ( $i\text{-C}_4\text{H}_{10}$ ) exhibit clear maxima in late winter and minima in late summer (Figures 1a–1f and Table 1). However, the question of how best to express the nonlinear process of air mass variability is a difficult one. We have chosen to calculate percentage variability employing a 10-point running average, where the value of each error bar represents the 1-sigma standard deviation of approximately 2 weeks worth of samples (Figure 1). We have also chosen to fit a sine curve to the data (Figures 1a–1f) as a visual guide to the seasonal trend, consistent with previous work [*Blake and Rowland*, 1986; *Jobson et al.*, 1994a; *Sharma et al.*, 2000]. Our best estimates of the annual maximum and minimum concentrations for each species over the year are presented in Table 1.

[13] To facilitate data usage and comparisons, numerical presentation of the data as monthly averages is also made in Table 2. The relative variability for the NMHCs fluctuated over the season, but tended to be lowest in fall and winter (Table 2). Average variability over the entire annual period was 8.9, 24, 20, 36, and 41% for ethane, propane, ethyne, *n*-butane, and *i*-butane, respectively.

[14] The seasonal measurements yielded good  $r^2$  values for the Pearson's least squares coefficients for the best fit sine curves for ethane, propane, ethyne, *n*-butane, and *i*-butane, of 0.95, 0.91, 0.91, 0.84, and 0.83, respectively (Figure 1). Ethane levels reached a seasonal minimum on 25 August ( $\pm 10$  days) and a maximum on 24 February ( $\pm 10$  days) (Figure 1a and Table 1). Ethane is the only NMHC that conforms to a continuous sinusoidal oscillation (Figure 1a). Its relative standard deviation from the best fit sine curve averages 6%, which is slightly lower than its average deviation from the running mean (8.9%).

[15] The shorter-lived gases propane, *i*-butane, *n*-butane, and ethyne deviate from a sinusoidal oscillation by exhibiting prolonged periods of relatively constant mixing ratios during summer (Figure 1). They peak earlier in winter (Table 1) and exhibit longer periods of low summer values in correlation with shorter lifetimes. These gases are more closely approximated with polynomial curves (fifth order), or with separate linear integrals for their fall increase, spring decay, and summer steady state.

[16] Levels of the short-lived *n*- and *i*-butanes (5.5 and 5.7 day summer lifetimes, respectively, Table 1) drop quickly during May, and by early June their mixing ratios are below 20 and 10 pptv, respectively. Thus their low summer concentrations are reached earliest and last longest. Concentrations tend to remain above their detection limit (DL) through the summer, except during August when most samples fall below 1 pptv. The medium-lived species propane and ethyne (14 and 19 day summer lifetimes, respectively, Table 1) reach low levels of about 95 and 113 pptv, respectively, in early June but remain well above their DLs throughout summer (Figures 1b and 1c). Ethyne



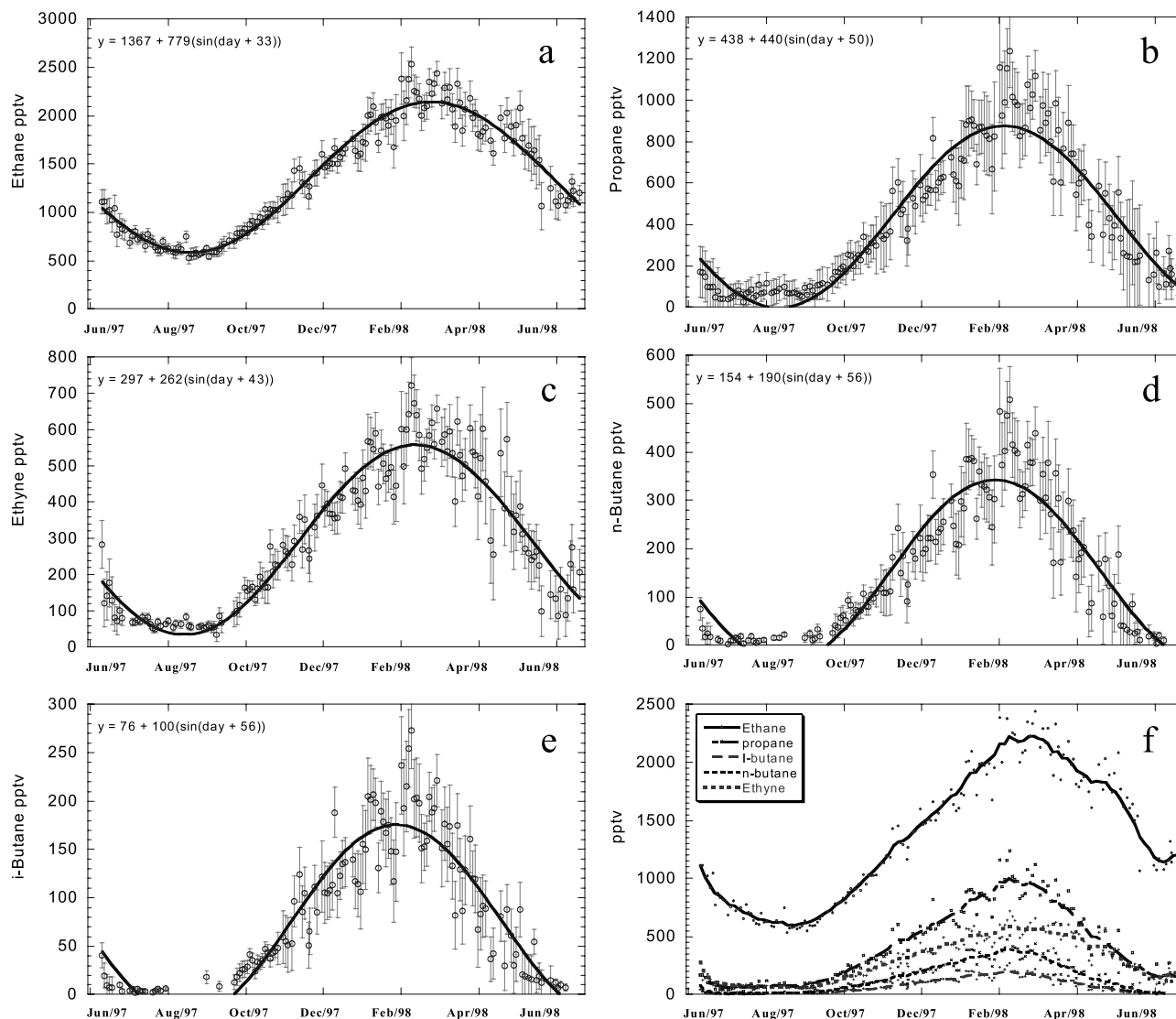


**Figure 1.** (a-f) C<sub>2</sub>-C<sub>4</sub> NMHC seasonal trends. The value of each error bar represents the 1-sigma standard deviation of a 10-point running average (approximately 2 weeks worth of samples). Each line is the best fit sinusoidal curve using least squares regression. Figure 1f shows all C<sub>2</sub>-C<sub>4</sub> NMHCs fitted with a smooth trend.

gradually declines to a minimum of about 55–60 pptv by 10–31 August. Propane declines to a minimum of 40 pptv for the period 24 June to 6 July, then rises back to a near-constant, or steady-state, concentration around 70 pptv through August.

[17] The fact that the butanes remain above DL in such a remote location, and that propane and ethyne do not decline below certain minimum levels in summer, led us to suspect some influence from local camp emissions. Propane and the butanes have a source in the liquid propane gas used for camp heating and cooking, while ethyne is the primary NMHC emission from the diesel generator, which powers the camp. Light NMHCs are also emitted from the camp snowmobiles and heavy machinery (tractors and plows). These local sources are likely to occasionally impact NMHC levels and to make them very sensitive to local climatological conditions such as the stability of the surface boundary layer and stagnant winds. However, the summer

1997 samples were collected at least 300 m upwind from the camp, typically when the wind strength was greater than  $2 \text{ m s}^{-1}$ , and care was taken to keep mobile source activities away from where they might influence sampling. A study of boundary layer conditions, wind direction, and wind speed, found no correlation with high summer values of ethyne, propane, or the butanes, so it is highly unlikely that these NMHC mixing ratios are the result of camp contamination. In addition, camp emissions are not significant enough to maintain the mixing ratios of ethyne and propane observed. Therefore the steady-state concentrations of these gases likely represent true background mixing ratios, the result of a balance between transport time from source regions, lifetime, and dilution.

[18] Summer to winter ratios of NMHCs have often been used to infer a local OH concentration [Boudries *et al.*, 1994; Goldstein *et al.*, 1995a] or the presence of alternative oxidants such as the nitrate radical [Penkett *et al.*, 1993]. To

**Table 1.** Summer and Winter Lifetimes of NMHC and Alkyl Nitrates

Compound	Summer			Winter			Winter/Summer <sup>d</sup>
	Minimum, <sup>a</sup> pptv	Date, days	$\tau^b$ , days	Peak, <sup>a</sup> pptv	Date, $\pm 10$ days	$\tau^c$ , days	
<i>NMHC</i>							
Ethane	577 $\pm$ 28	Aug. 25 $\pm$ 10	73	2214 $\pm$ 142	Feb. 24	920	3.4
Propane	52 $\pm$ 17	July 6 +60/-20	14	1012 $\pm$ 141	Feb. 10	160	22
Ethyne	55 $\pm$ 13	Aug. 29 +10/-20	19	594 $\pm$ 74	Feb. 11	220	11
<i>n</i> -Butane	13 $\pm$ 7	June 14–Sept. 8	5.5	408 $\pm$ 67	Feb. 8	59	82
<i>i</i> -Butane	5.7 $\pm$ 5.2	June 14–Sept. 8	5.7	208 $\pm$ 39	Feb. 8	60	83
<i>Alkyl Nitrates</i>							
Methyl	2.7 $\pm$ 0.5	Sept. 4 +10/-30	20	4.9 $\pm$ 0.4	Jan. 13	1500	1.9
Ethyl	2.5 $\pm$ 0.4	Sept. 4 +10/-60	12	5.7 $\pm$ 0.9	Jan. 23	890	2.3
<i>n</i> -Propyl	0.4 $\pm$ 0.2	Aug. 17 +20/-10	9.5	2.1 $\pm$ 0.6	Jan. 3–Feb. 2	550	4.8
<i>i</i> -Propyl	1.1 $\pm$ 0.4	July 12 $\pm$ 15	9.0	9.6 $\pm$ 0.8	Feb. 8	410	9.1
2-Butyl	1.4 $\pm$ 1.0	July 14 $\pm$ 10	6.2	13 $\pm$ 1.3	Feb. 22	480	9.2

<sup>a</sup>Minima and peak defined as running 10-point ( $\sim 2$  week) average and 1-sigma deviation.

<sup>b</sup>Summer lifetime calculated for reaction with OH =  $1 \times 10^6$  molecules per cubic centimeter [Spivakovsky *et al.*, 2000] and OH reaction rate constants from Atkinson *et al.* [1997], and photodissociation rate coefficients for C<sub>2</sub>–C<sub>4</sub> alkyl nitrates [Clemishaw *et al.*, 1997] and methyl nitrate [Tahukdar *et al.*, 1997] and an average temperature of 258 K.

<sup>c</sup>Winter lifetimes calculated same as for summer, but with OH =  $1 \times 10^5$  molecules per cubic centimeter [Spivakovsky *et al.*, 2000] and an average temperature of 243 K.

<sup>d</sup>Summer/winter ratios are calculated from the running 10-point winter peak values divided by the average summer values calculated from 500 summer samples collected from 1997 to 2000 as described in text.

obtain better statistics for our summer NMHC values, we combined the 1997–1998 results with those obtained from subsequent intensive summer campaigns conducted at Summit in 1999 and 2000, employing similar sampling and analytical methods. Average values for the nearly 500 combined summer samples are  $600 \pm 50$ ,  $45 \pm 20$ ,  $55 \pm 10$  pptv,  $5$  pptv  $\pm 100\%$  and  $2.5$  pptv  $\pm 200\%$  for ethane, propane, ethyne, *n*-butane, and *i*-butane, respectively. Using these best summer values and peak winter values from 1997 to 1998, we calculated winter/summer ratios for each

NMHC (Table 1). Because summer concentrations of the butanes may occasionally have been impacted by local camp emissions and the lowest true values were below the DL, winter/summer ratios for *i*- and *n*-butane (Table 1) are likely to be underestimated.

### 3.2. Alkyl Nitrates

[19] The alkyl nitrates, methyl (CH<sub>3</sub>ONO<sub>2</sub> or MeONO<sub>2</sub>), ethyl (C<sub>2</sub>H<sub>5</sub>ONO<sub>2</sub> or EtONO<sub>2</sub>), 2-propyl (2-C<sub>3</sub>H<sub>7</sub>ONO<sub>2</sub> or 2-PrONO<sub>2</sub>), 1-propyl (1-C<sub>3</sub>H<sub>7</sub>ONO<sub>2</sub> or 1-PrONO<sub>2</sub>), and

**Table 2.** Monthly Averages With 1-Sigma Standard Deviation for Summit

Compound	June	July	August	September	October	November
<i>NMHC</i>						
C <sub>2</sub> H <sub>6</sub>	1055 $\pm$ 146	698 $\pm$ 62	603 $\pm$ 51	684 $\pm$ 93	958 $\pm$ 92	1320 $\pm$ 142
C <sub>3</sub> H <sub>8</sub>	133 $\pm$ 64	63 $\pm$ 21	77 $\pm$ 18	124 $\pm$ 47	268 $\pm$ 51	453 $\pm$ 102
<i>i</i> -C <sub>4</sub> H <sub>10</sub>	12 $\pm$ 10	4 $\pm$ 1	ND	19 $\pm$ 7	40 $\pm$ 9	84 $\pm$ 28
<i>n</i> -C <sub>4</sub> H <sub>10</sub>	22 $\pm$ 20	10 $\pm$ 5	17 $\pm$ 3	33 $\pm$ 18	86 $\pm$ 20	159 $\pm$ 49
C <sub>2</sub> H <sub>2</sub>	149 $\pm$ 65	69 $\pm$ 10	62 $\pm$ 9	84 $\pm$ 38	193 $\pm$ 46	306 $\pm$ 64
<i>Alkyl Nitrate</i>						
CH <sub>3</sub> ONO <sub>2</sub>	3.97 $\pm$ 1.01	3.76 $\pm$ 0.84	2.97 $\pm$ 0.48	3.09 $\pm$ 0.65	3.96 $\pm$ 0.39	4.25 $\pm$ 0.43
C <sub>2</sub> H <sub>5</sub> ONO <sub>2</sub>	3.59 $\pm$ 0.87	2.88 $\pm$ 0.66	2.86 $\pm$ 0.51	2.91 $\pm$ 0.56	3.73 $\pm$ 0.34	4.23 $\pm$ 0.54
<i>i</i> -C <sub>3</sub> H <sub>7</sub> ONO <sub>2</sub>	2.38 $\pm$ 0.79	1.26 $\pm$ 0.56	2.16 $\pm$ 0.34	3.60 $\pm$ 1.25	5.67 $\pm$ 0.92	7.02 $\pm$ 0.57
<i>n</i> -C <sub>3</sub> H <sub>7</sub> ONO <sub>2</sub>	0.64 $\pm$ 0.19	ND	0.50 $\pm$ 0.25	0.53 $\pm$ 0.19	0.92 $\pm$ 0.23	1.35 $\pm$ 0.29
2-C <sub>4</sub> H <sub>9</sub> ONO <sub>2</sub>	1.80 $\pm$ 1.16	1.52 $\pm$ 0.98	1.74 $\pm$ 0.75	3.44 $\pm$ 2.02	5.50 $\pm$ 1.15	7.94 $\pm$ 1.15
Sum C <sub>1</sub> –C <sub>4</sub>	12.02 $\pm$ 2.92	9.43 $\pm$ 2.22	10.00 $\pm$ 2.07	13.57 $\pm$ 4.18	19.78 $\pm$ 2.70	24.20 $\pm$ 3.13
Compound	December	January	February	March	April	May
<i>NMHC</i>						
C <sub>2</sub> H <sub>6</sub>	1581 $\pm$ 89	1939 $\pm$ 180	2235 $\pm$ 160	2110 $\pm$ 149	1827 $\pm$ 118	1608 $\pm$ 281
C <sub>3</sub> H <sub>8</sub>	614 $\pm$ 80	838 $\pm$ 120	1001 $\pm$ 117	819 $\pm$ 125	492 $\pm$ 122	293 $\pm$ 113
<i>i</i> -C <sub>4</sub> H <sub>10</sub>	123 $\pm$ 23	174 $\pm$ 33	201 $\pm$ 35	138 $\pm$ 31	64 $\pm$ 25	29 $\pm$ 24
<i>n</i> -C <sub>4</sub> H <sub>10</sub>	238 $\pm$ 45	338 $\pm$ 61	395 $\pm$ 57	279 $\pm$ 66	133 $\pm$ 55	53 $\pm$ 51
C <sub>2</sub> H <sub>2</sub>	400 $\pm$ 38	505 $\pm$ 61	596 $\pm$ 68	541 $\pm$ 59	430 $\pm$ 118	256 $\pm$ 84
<i>Alkyl Nitrate</i>						
CH <sub>3</sub> ONO <sub>2</sub>	4.54 $\pm$ 0.39	4.93 $\pm$ 0.43	4.38 $\pm$ 0.43	4.27 $\pm$ 0.50	4.28 $\pm$ 1.48	3.09 $\pm$ 0.36
C <sub>2</sub> H <sub>5</sub> ONO <sub>2</sub>	4.70 $\pm$ 0.63	5.64 $\pm$ 0.85	4.99 $\pm$ 0.85	4.96 $\pm$ 0.65	5.37 $\pm$ 1.96	4.27 $\pm$ 0.62
<i>i</i> -C <sub>3</sub> H <sub>7</sub> ONO <sub>2</sub>	7.96 $\pm$ 0.49	9.13 $\pm$ 0.89	9.49 $\pm$ 0.82	9.02 $\pm$ 0.93	8.36 $\pm$ 1.54	5.29 $\pm$ 1.28
<i>n</i> -C <sub>3</sub> H <sub>7</sub> ONO <sub>2</sub>	1.79 $\pm$ 0.71	1.91 $\pm$ 0.40	1.82 $\pm$ 0.49	1.84 $\pm$ 0.57	1.60 $\pm$ 0.61	0.96 $\pm$ 0.26
2-C <sub>4</sub> H <sub>9</sub> ONO <sub>2</sub>	9.38 $\pm$ 1.20	11.23 $\pm$ 1.72	12.58 $\pm$ 1.13	11.44 $\pm$ 1.62	9.67 $\pm$ 1.73	5.35 $\pm$ 1.56
Sum C <sub>1</sub> –C <sub>4</sub>	26.97 $\pm$ 3.04	32.07 $\pm$ 4.34	32.82 $\pm$ 3.42	31.28 $\pm$ 3.89	28.99 $\pm$ 6.89	18.95 $\pm$ 3.18

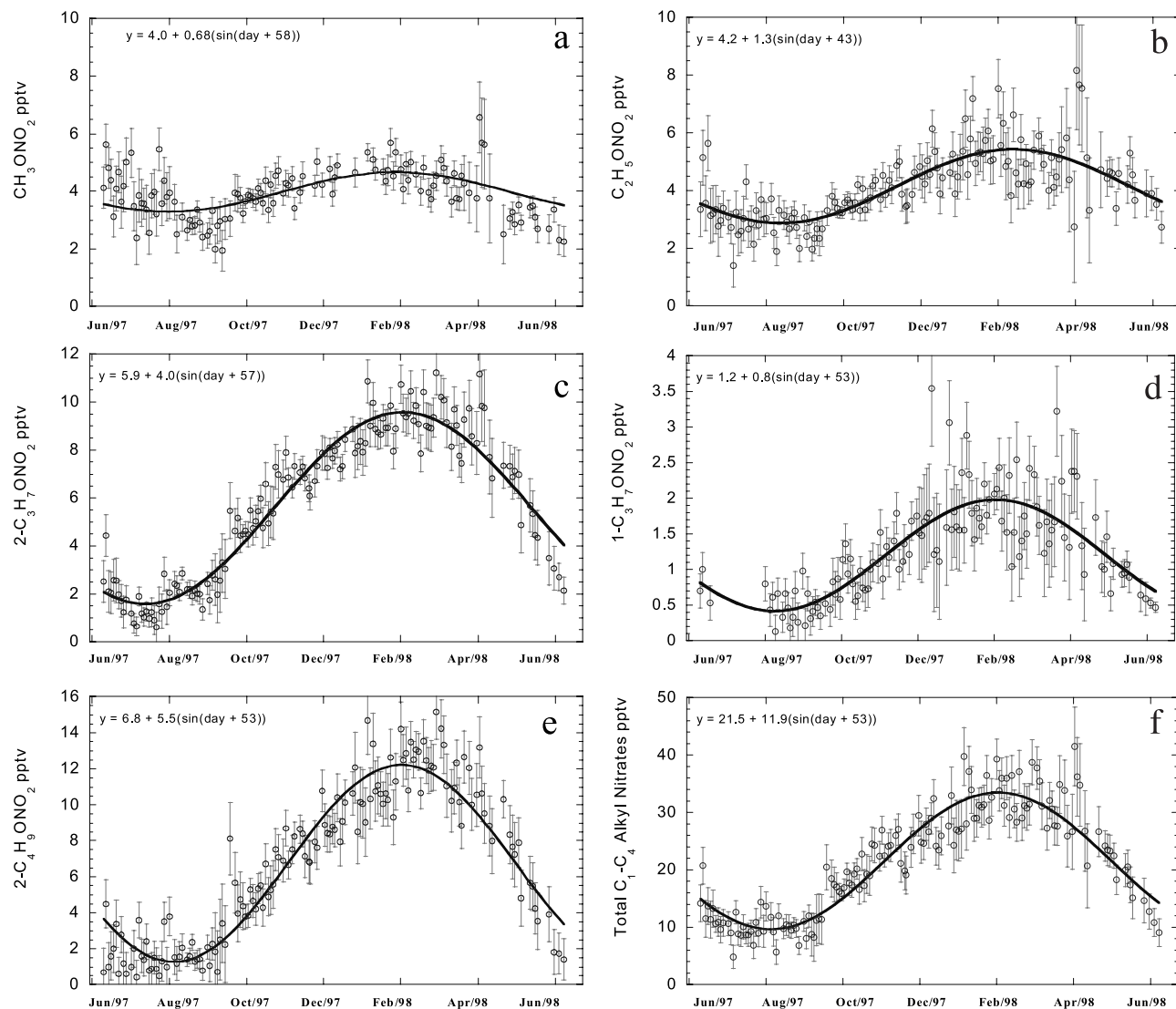


**Figure 2.** (a–f)  $C_1$ – $C_4$  alkyl nitrate seasonal trends with error bars representing the 1-sigma standard deviation of a 10-point running average. Each alkyl nitrate is then fit to a sinusoidal curve using least squares regression.

2-butyl nitrate ( $2-C_4H_9ONO_2$  or 2-BuONO<sub>2</sub>), all exhibit seasonal oscillations similar to the NMHCs (Figures 2a–2e). The sum of these  $C_1$ – $C_4$  alkyl nitrates is also presented (Figure 2f). The seasonal variations are illustrated in the same fashion as for the NMHCs, with 1-sigma standard deviations for each sample point calculated from 10-point running averages, and fit to sinusoidal curves (Figure 2). The  $r^2$  values for the fits of the data to the sine curves are 0.31, 0.58, 0.64, 0.90, 0.89, and 0.86 for  $CH_3ONO_2$ ,  $C_2H_5ONO_2$ ,  $1-C_3H_7ONO_2$ ,  $2-C_3H_7ONO_2$ ,  $2-C_4H_9ONO_2$ , and total  $RONO_2$ , respectively.

[20] A small seasonal methyl nitrate variation with an approximate winter to summer ratio of 1.9 (Table 1) is observed. Of the alkyl nitrates, methyl nitrate shows the lowest percentage variability over the seasonal study averaging 15% (Figure 2a). Ethyl nitrate mixing ratios remained within a similar concentration range, but demonstrated a clearer seasonal cycle, with a minimum of  $2.5 \pm 0.4$  pptv around 4 September (+10/–60 days) and a maximum of  $5.7 \pm 0.9$  pptv around the beginning of February (winter/summer

ratio 2.3) (Figure 2b and Table 1). The compounds 1-propyl, 2-propyl, and 2-butyl nitrate display successively stronger seasonal cycles, with winter to summer ratios of 4.8, 9.1, and 9.2, respectively (Table 1).

[21] The shorter-lived alkyl nitrates peak later in the winter than the longer-lived alkyl nitrates (Table 1), the reverse pattern to that seen for the NMHCs. In addition, peak levels of longer-lived 2-butyl nitrate and 2-propyl nitrate are well correlated with butane and propane, respectively, while ethyl nitrate is poorly correlated with ethane. (The Pearson's least squares correlation coefficients for  $2-C_3H_7ONO_2$  versus  $C_3H_8$ , and  $2-C_4H_9ONO_2$  versus  $n-C_4H_{10}$  are 0.84 and 0.81, respectively, while that for  $C_2H_5ONO_2$  versus  $C_2H_6$  is only 0.59.) The fact that the winter maxima of the shorter-lived alkyl nitrates are closely linked to those of their parent NMHCs is consistent with the principal source of these gases being secondary production from the parent hydrocarbons. The poor ethyl nitrate/ethane correlation is in accordance with the principal  $C_1$ – $C_2$  alkyl nitrate sources being primary rather than secondary, and the

timing of their winter maxima being dominated by sources other than NMHCs.

[22] Total C<sub>1</sub>–C<sub>4</sub> alkyl nitrates maximize in winter at an average value of about  $33.9 \pm 3.5$  pptv (Figure 2f). The 2-propyl and 2-butyl nitrates dominate this winter total, representing more than 60%. During summer, when total alkyl nitrate mixing ratios are much lower than in winter (at approximately  $10 \pm 2$  pptv, Figure 2f) contributions from methyl and ethyl nitrate are dominant.

## 4. Discussion

### 4.1. Comparison of NMHCs With Published Data

[23] In Figures 3a–3d, we compare the average mixing ratios for ethane, propane, ethyne, and *n*-butane at Summit (72.57°N) to those previously reported in the latitude range 42°–72°N (Harvard Forest, Massachusetts, 42.54°N [Goldstein *et al.*, 1995a], Fraserdale, Canada, 50°N [Jobson *et al.*, 1994a], Rorvik, Sweden, 57.23°N [Lindskog and Moldanova, 1994], North Atlantic Ocean, ~58°N [Penkett *et al.*, 1993], Utö Island, Baltic Sea, Finland, 59.47°N, and Pallas, northern Finland, 67.58°N [Laurila and Hakola, 1996], and Barrow, Alaska, 71.17°N (D. Blake, personal communication, unpublished data). A seasonal study of ethane measured at multiple points in Alaska from 65° to 70°N between 1983 and 1985 is also included [Blake and Rowland, 1986].

[24] The two Alaskan data sets were produced from our laboratory here at UCI, so they are calibrated to the same scale as the Summit data. The data from Barrow are the averages of samples collected in March, June, September, and December from 1996 to 2000 (D. Blake, personal communication, unpublished data). The data from Jobson *et al.* [1994a] have been used many times in comparisons of NMHC seasonal trends [Bottenheim and Shepherd, 1995; Rudolph, 1995; Poisson *et al.*, 2000; Sharma *et al.*, 2000]. The mean summer and winter extremes for April 1990 to October 1992 for these data are plotted in Figure 3. The other data sets are all seasonal studies with various temporal resolutions, which we have simplified to monthly means for ease of comparison. The seasonal trend from Goldstein *et al.* [1995a] represents background concentrations measured at Harvard Forest, defined as the samples with the lowest 10% mixing ratios. Their data set is of unusually high resolution (900 samples per month from August 1992 to July 1994), and the low-latitude location of Harvard Forest (42.54°N) puts it within the continental United States source region. We have converted the Penkett *et al.* [1993] data to monthly averages (multiple years or duplicate data points within a month were combined when present) of samples collected aboard a small aircraft over the North Atlantic Ocean from January 1987 to April 1989 approximately once to twice per month. The authors separated the data between low altitude (~150 m) and the free troposphere (up to 3300 m). We have plotted the low-altitude averages for consistency in comparing with the other surface sites. The data from Rorvik, Sweden, 57.23°N by Lindskog and Moldanova [1994] are the monthly average of measurements collected every 4 hours from February 1989 to October 1990. The data from Utö Island in the Baltic Sea, near Finland, 59.47°N, and at Pallas, northern Finland, 67.58°N, were collected once every 2 days from January 1993 to December 1994 and twice weekly from January 1994 to December

1994, respectively [Laurila and Hakola, 1996]. All sites are considered remote from urban or anthropogenic inputs and were presented as background concentrations for their specific region.

[25] Similar to comparisons made by Rudolph [1995], we find good agreement between high-latitude NH ethane data reported by the various measurement groups (Figure 3). Maximum winter ethane values for all nine data sets (covering a latitude range of 42°–72°N) lie within the range 2100–2700 pptv, with an average of  $2350 \pm 200$  pptv between February and March. This narrow winter range limits any spatial gradient over the geographical range of the various sampling sites, especially as this comparison does not take into account variability in analytical precision or accuracy between the numerous measurement groups.

[26] In fact, it is possible that much of the remaining variability between data sets may be attributable to analytical differences. The NOMHICE tested the analytical abilities of some 20–50 international laboratories making NMHC measurements [Apel *et al.*, 1994]. Results from the analysis of whole air samples (Task 4), showed that deviation from the NIST and NCAR calibrated values can range from 10 to 50% between independent laboratories [Sive, 1998], making quantitative intercomparison of published data originating from different labs highly uncertain.

[27] However, the UCI measurements deviated from NIST values by only 1.4, 0.1, 8.0, 0.0, and 0.8% for ethane, propane, ethyne, *n*-butane, and *i*-butane, respectively [Sive, 1998]. The Harvard measurement group also achieved a better than 10% deviation for this same test [Goldstein *et al.*, 1995b], with absolute deviations of only a few percent for the alkanes and a maximum of 10% deviation for ethyne (A. H. Goldstein, personal communication, 2002). This indicates that the Harvard Forest results are quantitatively comparable to the UCI measurements. The comparison will remain qualitative in nature for the other data sets.

#### 4.1.1. Temporal Trends

[28] Long-term trends are another possible cause of systematic difference between the data sets shown in Figure 3. Ethane above the Jungfraujoch station in Switzerland increased at a rate of  $0.85\% \text{ yr}^{-1}$  from 1951 to 1988 [Ehhalt *et al.*, 1991], but decreased at  $-1.20 \pm 0.65\% \text{ yr}^{-1}$  from 1995 to 1999 [Rinsland *et al.*, 2000]. Total column ethane also decreased at Kit Peak, Colorado at  $-0.64 \pm 0.79\% \text{ yr}^{-1}$  from 1977 to 1997 [Rinsland *et al.*, 1998]. Thus average NH ethane appears to have increased from 1951 to 1988 followed by a decrease from 1995 to 1999. However, there is no conclusive information covering the period from 1988 to 1995.

[29] The average winter maximum values and periods covered by the three most comparable (because they all originate from UCI) ethane data sets are:  $2050 \pm 200$  pptv, 1983–1985 (Alaska);  $2218 \pm 194$  pptv, 1996–1999, (Barrow); and  $2214 \pm 142$  pptv, 1997–1998 (Summit). All three winter averages are statistically equivalent, so no obvious temporal trend in ethane mixing ratios can be inferred from this analysis. However, a small secular trend (in the range of  $1\% \text{ yr}^{-1}$ ) could easily be obscured by the natural variability of NH mixing ratios, even over a 10-year time-scale.

#### 4.1.2. Spatial Gradients

[30] The three UCI data sets typically define the lower end of the concentration range for each NMHC (Figure 3).



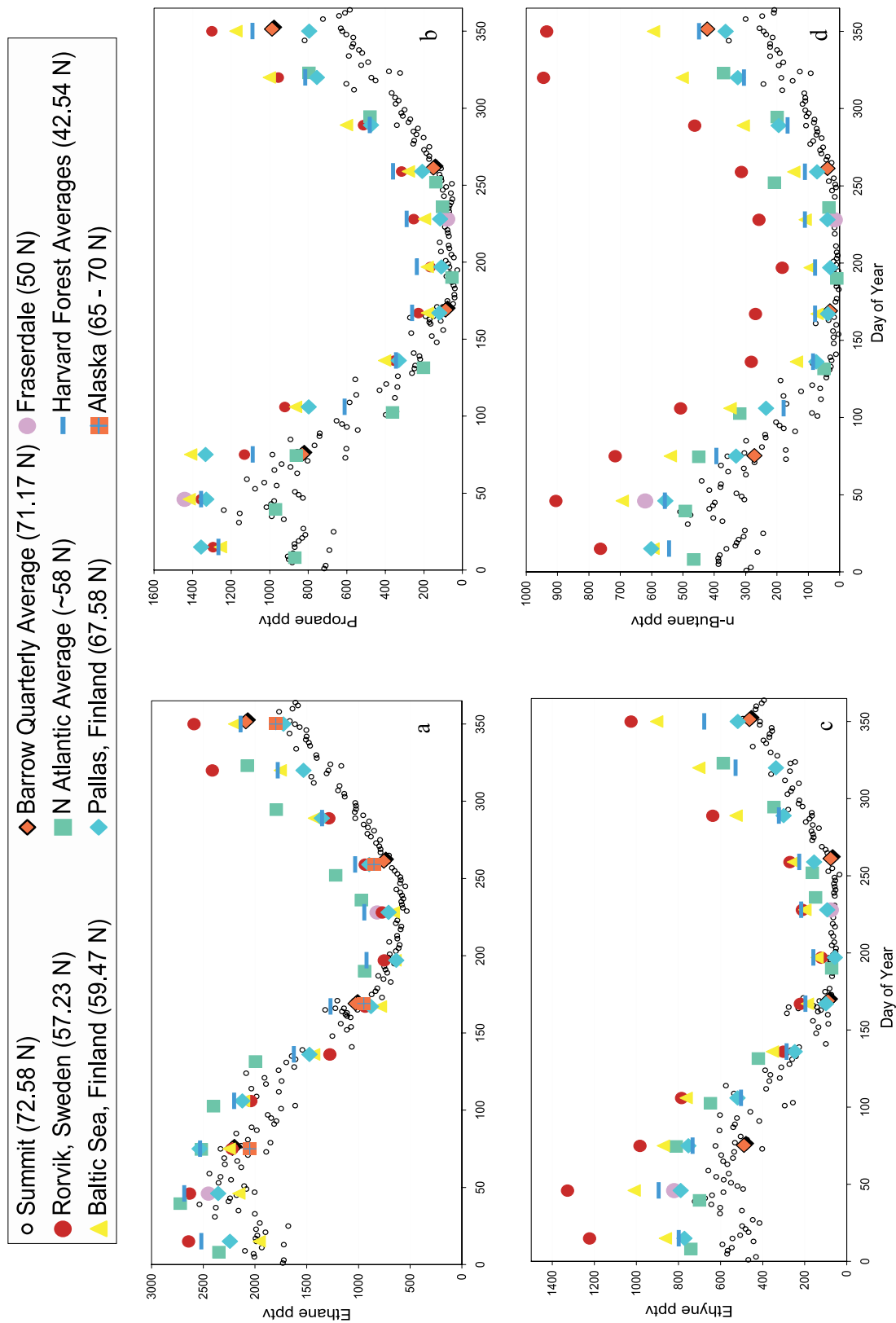


**Figure 3.** (a–d) Summit data plotted against published data and Barrow, AK. Harvard Forest [Goldstein *et al.*, 1995a] 0.1 Quartile of data, averaged monthly values for 1993–1994. N. Atlantic average [Penkett *et al.*, 1993] monthly averaged low-altitude data from 1988 to 1989. Frasierdale [Jobson *et al.*, 1994a] mean winter and summer concentrations reported for 1990–1992. Baltic Sea and Pallas, Finland [Laurila and Hakola, 1996] monthly averaged data for 1993–1994. Rorvik, Sweden [Lindsog and Moldanova, 1994] monthly averaged data from 1989 to 1990. Barrow, AK, (UCI, unpublished data) quarterly averaged data from 1996 to 1999. Alaska [Blake and Rowland, 1986] averaged quarterly data for ethane from 1983 to 1985.



This could reflect a trend of decreasing concentrations from the source regions between 40° and 60°N, or a difference in calibration (for data sets other than Harvard Forest). For ethane, the average mixing ratios at Harvard Forest (42°N) are higher than Summit (72°N) by approximately 200 and 600 pptv during summer and winter, respectively (or approximately  $22 \pm 9\%$  seasonally). This trend is inconsistent with the increasing concentrations with latitude to 60°–70°N in winter, and nearly flat latitude gradients in summer, reported by *Rudolph* [1995] and *Gupta et al.* [1998], respectively. Therefore the differences between the Harvard Forest and Summit sites are more likely to represent a latitudinal gradient caused by the proximity of Harvard Forest to continental source regions.

[31] In general, the shorter-lived NMHCs show higher variability between data sets than ethane. Again, the mixing ratios measured at Harvard Forest exceed those from Summit, this time by  $43 \pm 20$ ,  $38 \pm 19$ ,  $51 \pm 22$ , and  $49 \pm 19\%$  for propane, ethyne, *n*-butane, and *i*-butane, respectively, over the annual cycle. These differences are correlated with the respective OH rate constants for the NMHCs, but not linearly, probably indicating the effects of dilution of the more polluted air masses at the lower latitude site.

[32] Butane levels at Rorvik, Sweden (57.23°N) are greater than those for any other data set over the entire annual cycle, as are winter ethyne levels. These high levels could reflect local sources near the sampling site or a calibration difference, but the similarities of the seasonal patterns at Rorvik with those at the Baltic Sea site (on the other side of Sweden) argue for the influence of a large regionally dispersed source of the butanes.

[33] In general, NMHC measurements made at Barrow closely match Summit ( $r^2 = 0.99-1$ ) giving nearly identical monthly averages in March, June, and September, with the exception of the high alkane levels for December. Barrow is located at a latitude similar to Summit, so the similarities are consistent with assumed negligible longitudinal gradients (away from source regions) [*Kanakidou et al.*, 1991; *Rudolph*, 1995; *Blake et al.*, 2003a].

[34] Extended periods of high concentrations of atmospheric sulfate aerosol, known as Arctic Haze, originating from within Eurasia [*Barrie et al.*, 1994; *Klonecki et al.*, 2003], are well documented to influence Barrow's atmosphere in winter and spring [*Bodhaine et al.*, 1984]. It continues to be a feature of the Arctic troposphere [*Scheuer et al.*, 2003], even though it has decreased at Barrow since the mid-1980s [*Bodhaine and Dutton*, 1995]. By contrast, only brief episodes of high sulfate aerosol were documented at Summit during the 1997–1998 winter-over (J.-L. Jaffrezo et al., Seasonal variations in aerosol chemical species on the Greenland ice sheet, submitted to *Journal of Geophysical Research*, 2002). This points to the possibility that the relatively elevated December concentrations of NMHCs at Barrow might be associated with Arctic Haze. However, this would not explain why only the alkanes are elevated (not ethyne) and why NMHC mixing ratios are so similar in spring when Arctic Haze is most common [*Bodhaine and Dutton*, 1995].

[35] Barrow is at sea level, while Summit is located at an altitude of 3 km, raising questions about the possible effect of altitude to explain the December differences. The similarity between Barrow and Summit during most of the year

indicates that Summit typically is representative of a surface site, i.e., influenced most strongly by boundary layer air rather than the free troposphere. Recently, 0–8 km vertical profiles from the Arctic during the 1999–2000 TOPSE airborne campaign revealed strong vertical winter gradients, with a relatively well-mixed lower atmosphere to 3 km, persisting until about the spring equinox [*Blake et al.*, 2003a]. A particularly strong vertical gradient at altitudes below 3 km during December may explain the relatively low levels observed at Summit, however, this again does not explain the agreement with ethyne. A third possibility is that local or regional emissions influence the Barrow sampling site more strongly in December. This possibility is discussed later.

#### 4.1.3. Comparison Summary

[36] In summary, our comparison of NMHC data sets demonstrates that the C<sub>2</sub>–C<sub>4</sub> NMHC mixing ratios at Summit define the lower limits in the range of background mixing ratios of NMHCs within the mid- to high-latitude NH over a seasonal cycle. The Summit data set is comparable with other NH seasonal data sets, but it exhibits an effectively smooth seasonal variation with low biweekly variability, while other data sets are typically more influenced by local and regional continental sources. No statistically significant secular trend can be determined from the comparison of UCI data sets from 1983 to 1997, although it is possible that any trend is obscured by natural variability. Evidence for a latitudinal gradient between 40° and 70°N is inconsistent with previously reported latitudinal trends, possibly again reflecting the more remote nature of the Summit site compared to other sites.

#### 4.2. Seasonal Trends and Photochemical Removal

[37] Its position in central Greenland puts Summit in the direct path for long-range transport originating from the major NH industrialized regions of North America, Europe, and Asia [*Kahl et al.*, 1997, 1999]. Transport climatology reported by *Kahl et al.* [1997, 1999] indicates that dominant source regions that impact Summit have a distinct seasonal pattern. Wintertime circulation is more vigorous, with nearly 30% of all 10-day back trajectories reaching back to the North Pacific or Eurasia. Summertime trajectories tend to be shorter, with the dominant source region being North America (40°–85°N) while only about 10% reach back to eastern Asia within 10 days. Thus we would expect lower mixing ratios of NMHCs in summer due to much weaker transport from source regions, combined with increased photochemistry. Indeed, this is what is seen in chemical transport models using hypothetical short- and long-lived tracers to mimic the seasonality of the NMHCs in the high latitudes [*Klonecki et al.*, 2003]. However, the strong buildup of NMHC mixing ratios in the winter at high latitudes is not solely a result of transport, but also a consequence of seasonally changing photochemistry as evidenced by the seasonal trends within the source regions themselves at midlatitudes such as the Harvard Forest [*Goldstein et al.*, 1995a], the southeastern United States at 31°–35°N [*Hagerman et al.*, 1997], and Happo, Japan at 36°41'N [*Sharma et al.*, 2000].

[38] In order to examine influences affecting seasonal variations of the NMHCs at Summit, we have applied an analysis using hydrocarbon ratios, which has been used to

determine the photochemical age of an air mass [Nelson and Quigley, 1982; Roberts *et al.*, 1984, 1985; Rudolph and Johnen, 1990; Parrish *et al.*, 1992; McKeen *et al.*, 1996], and the dominance of OH oxidation [Jobson *et al.*, 1994a; Bottenheim and Shepherd, 1995]. The analysis is based on the assumption that the ratio of the concentration of two species can be used to characterize the age of an air mass from the specific point in time when those two species were simultaneously introduced into that air mass. This requires that the species be removed by photochemical reactions that follow pseudo first-order kinetics of significantly different rates and that any dilution is with surrounding air masses that contain negligible concentrations of those species with no further emissions [Rudolph and Johnen, 1990; Parrish *et al.*, 1992]. For long-range transport, dilution cannot be neglected due to nonnegligible concentrations of the longer-lived species, which will bias the determination of age, as has been shown by McKeen and Liu [1993]. However, the calculation still offers insight into the NMHCs removal processes. If dilution effects are neglected, then the concentration of an alkane can be expressed as

$$[R] = [R]_0 \exp(-k_R[\text{OH}]_{\text{ave}}t) \quad (1)$$

where  $[R]_0$  and  $[R]$  are the concentrations of alkane initially and at the sampling time, respectively,  $k_R$  is the bimolecular rate constant for reaction of the alkane (R) with OH,  $[\text{OH}]_{\text{ave}}$  is the time averaged OH concentration, and  $t$  is the time from emission to sampling. The ratio of the two alkanes, ethane (E) and propane (P), is then

$$\ln([P]/[E]) = \ln([P]_0/[E]_0) - (k_P - k_E)[\text{OH}]_{\text{ave}}t \quad (2)$$

Using an estimated  $[\text{OH}]_{\text{ave}}$  concentration, the relative age of any two samples can be estimated, but in practice this calculation is dependent on a temporally fluctuating OH concentration as well as the effects of dilution. Expanding this analysis to three alkanes; ethane, propane, and butane (B) emitted simultaneously into an air parcel and removed by OH oxidation allows the elimination of the dependence on  $[\text{OH}]_{\text{ave}}$ . Equation (2) is combined for butane/ethane and propane/ethane to give

$$\ln([B]/[E]) = M\{\ln([P]/[E])\} + D \quad (3)$$

where the slope  $M$  is given by

$$M = (k_B - k_E)/(k_P - k_E) \quad (4)$$

and the intercept  $D$  is given by

$$D = \ln([B]_0/[E]_0) - M\{\ln([P]_0/[E]_0)\} \quad (5)$$

[39] Figure 4a shows the correlation between the natural logarithm of *n*-butane/ethane versus propane/ethane for the annual sampling period at Summit. The slope of the correlation is 1.58 ( $r^2 = 0.83$ ), in close agreement with data reported by Rudolph and Johnen [1990], Parrish *et al.* [1992], Jobson *et al.* [1994a], and Bottenheim and Shepherd [1995] who reported slopes of 1.66 ( $r^2 = 0.71$ ), 1.47 ( $r^2 = 0.90$ ), 1.44 ( $r^2 = 0.92$ ), and 1.42 ( $r^2 = 0.69$ ), respectively. All the slopes for the literature data above, and for Summit,

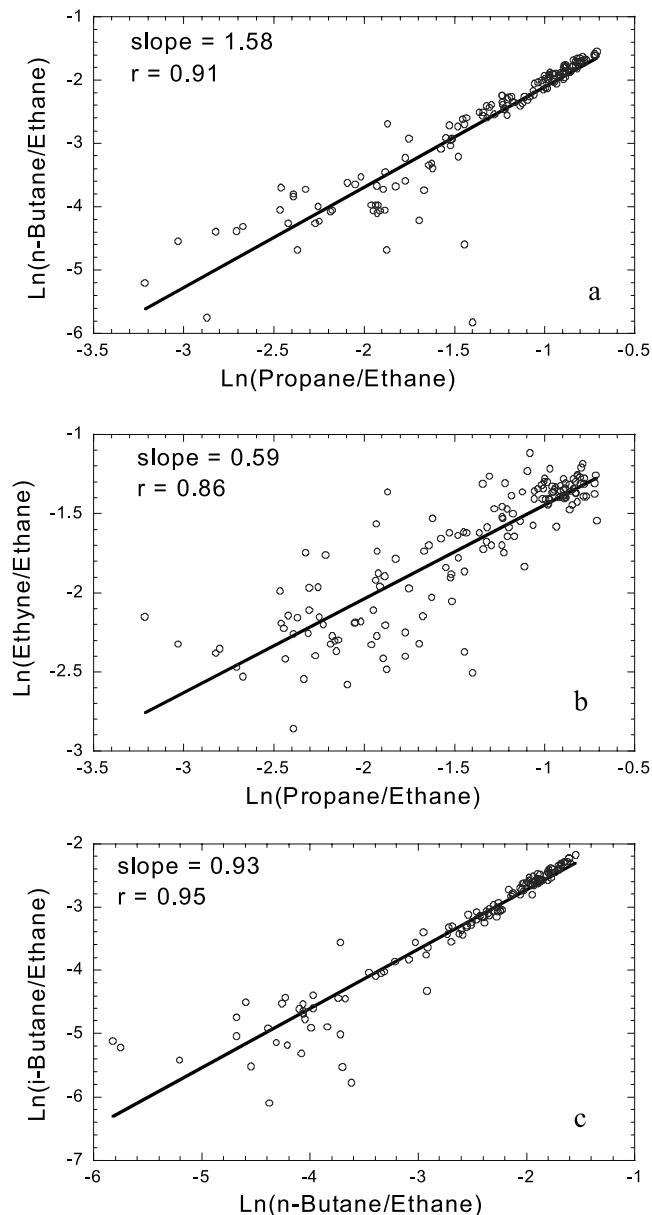


**Figure 4.** (a)  $\ln(n\text{-butane/ethane})$  to  $\ln(\text{propane/ethane})$ , (b)  $\ln(\text{ethyne/ethane})$  to  $\ln(\text{propane/ethane})$ , and (c)  $\ln(i\text{-butane/ethane})$  to  $\ln(n\text{-butane/ethane})$ . Winter values are in upper right corner and summer values in lower left.

fall below the kinetic value of 2.97 (for  $(k_{n-B} - k_E)/(k_P - k_E)$ ) at 243 K, the annual average temperature at Summit). This is consistent with the effects of dilution [Parrish *et al.*, 1992; McKeen and Liu, 1993; McKeen *et al.*, 1996], which will cause the slope of the linear fit to decrease when diluting air contains relatively higher concentrations of ethane versus propane and *n*-butane.

[40] Figures 4b and 4c show the natural log plot correlations for propane/ethane versus ethyne/ethane and *i*-butane/ethane versus *n*-butane/ethane following equation (2). As suggested by Jobson *et al.* [1994a], correlations between NMHCs with similar OH rate constants minimizes the effect of dilution because any diluting air will maintain the same ratio. The slope of  $\ln(\text{ethyne/ethane})$  to  $\ln(\text{propane/ethane})$

is 0.59 ( $r^2 = 0.74$ ) while the kinetic ratio is 0.66 at 243 K. The slope of  $\ln(i\text{-butane/ethane})$  to  $\ln(n\text{-butane/ethane})$  is 0.93 ( $r^2 = 0.90$ ) and the kinetic ratio is 0.98 at 243 K. These results are in good agreement with *Jobson et al.* [1994a] and *Bottenheim and Shepherd* [1995], who calculated 0.97 ( $r^2 = 0.91$ ) and 0.75 ( $r^2 = 0.83$ ), for  $\ln(i\text{-butane/ethane})$  to  $\ln(n\text{-butane/ethane})$  and 0.66 ( $r^2 = 0.68$ ) and 0.66 ( $r^2 = 0.42$ ) for  $\ln(\text{ethyne/ethane})$  to  $\ln(\text{propane/ethane})$ , respectively. There is a slight temperature dependence, raising the kinetic ratio of  $(k_{i-B} - k_E)/(k_{n-B} - k_E)$  from 0.94 to 0.98 with decreasing temperature from 273 to 243 K, which is negligible compared to the variability of the data. This analysis does not allow for the separation of dilution from photochemical removal, and thus does not enable the characterization of air mass age. However, the excellent agreement of observational measurements to kinetic rate constants is a strong indication that NMHC removal process, and therefore seasonal trends at Summit, are dominated by reaction with OH.

[41] The observation that the empirical value of the  $\ln(n\text{-butane/ethane})$  versus  $\ln(\text{propane/ethane})$  slope falls below the kinetic value was suggested to be an indication of chlorine (Cl) chemistry removal [*Finlayson-Pitts*, 1993; *Jobson et al.*, 1994b; *Bottenheim and Shepherd*, 1995], as well as the effect of dilution [*Parrish et al.*, 1992; *McKeen and Liu*, 1993; *McKeen et al.*, 1996]. To examine the possible influence of Cl oxidation, the ratio of  $i\text{-butane}/n\text{-butane}$  is plotted against  $n\text{-butane}$  (Figure 5) [*Jobson et al.*, 1994b]. Because Cl reacts more readily with  $n\text{-butane}$  than with  $i\text{-butane}$ , an increase from its average ratio close to 0.55 indicates influence from Cl radicals. Although scatter in the  $i\text{-butane}/n\text{-butane}$  ratio can be seen when the butane mixing ratios fall below 40 pptv (possibly as the result of camp emissions and/or by higher measurement variability as the mixing ratios approach their DL), the  $i\text{-butane}/n\text{-butane}$  ratio at Summit remain steady at approximately 0.51 (Figure 5), indicating that OH oxidation is the most important butane removal process.

[42] Bromine (Br) oxidation is another possible influence on NMHC mixing ratios. Ethyne reacts much faster with Br than do the alkanes, so the fact that the seasonal trend of ethyne closely follows the behavior of the other NMHCs rules out any large Br influence.

[43] The halogens, Br and Cl, are primarily considered to be important oxidants of NMHCs in the MBL, where sea salt can lead to high concentrations of these radical species [*Rudolph et al.*, 1996]. Thus we did not expect significant halogen oxidant chemistry at Summit based on its location remote from sea salt influence. The TOPSE campaign demonstrated that halogen chemistry in the Arctic is primarily limited to sites near the ocean and within the boundary layer (<1 km) where ozone depletion events (ODE) were encountered [*Ridley et al.*, 2003]. While Summit NMHC concentrations correlate with 0–3 km concentrations during TOPSE [*Blake et al.*, 2003a] and surface sites in Barrow, Alaska (as shown previously), they are distinct from depletions of NMHCs encountered near the Arctic Ocean during ODEs (B. C. Sive et al., Non-methane hydrocarbon and halocarbon measurements made over the Arctic and high northern latitudes: Impact of halogen chemistry on Arctic lower tropospheric ozone, submitted to *Journal of Geophysical Research*, 2002). This

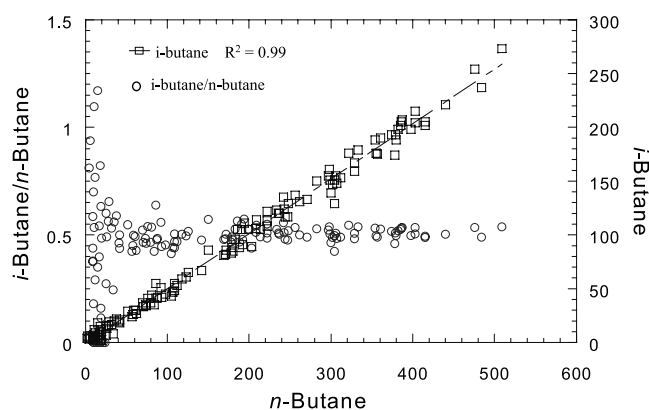


**Figure 5.** Iso-butane/ $n$ -butane to  $n$ -butane exhibits no significant evidence for chlorine chemistry.

suggests that Arctic surface air does not often reach Summit, in general agreement with the average back trajectories for Summit, which typically take zonal or southern approaches to Summit [*Kahl et al.*, 1997]. We did not have ozone data for Summit during this project, so we were unable to evaluate any possible ODEs based on ozone mixing ratios, but current measurements may be able to identify if ODEs influence the Summit site.

### 4.3. Estimating Source Emission Ratios in the Northern Hemisphere

[44] At Summit, the low variability of the seasonal cycle suggests that, being so far removed from regional sources, Summit is receiving well-mixed high-latitude NH air. The data collected at remote Arctic sites such as Barrow (Figure 3) and the Ny-Ålesund International Arctic Environmental Research and Monitoring Station, Svalbard, in the Arctic sea [*Hov et al.*, 1984, 1989; *Solberg et al.*, 1996] are of comparably low variability, presumably for the same reason. However, we have seen that Summit tends to avoid most influence from Arctic Haze, as well as the oxidative chemistry associated with sea salt influence (Br and Cl radical chemistry). Thus Summit is an ideal location to study the changing Arctic environment caused by anthropogenic influences and climatic change.

[45] *Penkett et al.* [1993] inferred a latitudinally and longitudinally well-mixed free troposphere at middle to high northern latitudes by demonstrating the reproducibility of the amplitude of the seasonal variation for NMHCs from year to year. This reproducibility was also shown in our earlier comparison with previously published data (Figure 3).

[46] Due to low levels of OH during winter [*Spivakovskiy et al.*, 2000] the lifetimes of the NMHCs (Table 1) are all much longer than the mid- to high-latitude interhemispheric mixing time ( $\sim 1\text{--}2$  months) [*Singh and Zimmerman*, 1992]. Because of the very low photochemical removal under these winter conditions, NMHC ratios are expected to differ from actual source emission ratios primarily due to dilution. To estimate the relative degree of photochemical aging, the ratio ethyne/CO can be used as a marker for fresh versus aged emissions. A value of around 3–4 represents fresh emissions and a value less than 1 is indicative of well-aged air [*Blake et al.*, 1996, 1999; *Smyth et al.*, 1996]. Figure 6 shows the seasonal trend from June 1997 to March



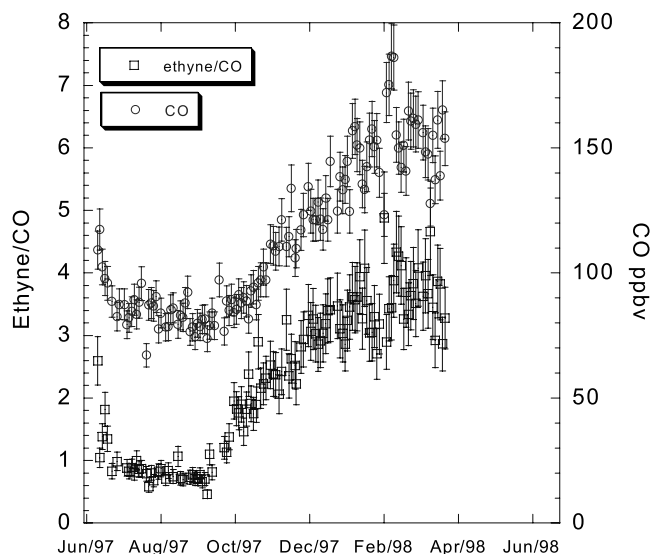


**Figure 6.** Seasonal trend of CO (open circles) plotted with ethyne/CO ratio (pptv/ppbv, open squares). Each month represents the first day of the month.

1998, for CO and the ethyne/CO ratio (pptv/ppbv). Ethyne/CO values at Summit during the January–February period are considered fresh at approximately 4 pptv/ppbv, consistent with the air masses reaching Summit without undergoing very much photochemical processing since their emission. This is also in agreement with measurements made during the TOPSE campaign between 58°–85°N and 0–3 km where ethyne/CO values were near 4 pptv/ppbv during February [Blake *et al.*, 2003a]. Therefore we postulate that well-mixed NH air reaching Summit during the winter should represent a useful average of high-latitude NH NMHC sources.

[47] To obtain a best estimate of emission ratios for the sources that impact Summit during the winter, we have taken the ratio of the slopes during their fall accumulation period (8 September to 8 February) when the correlations between individual NMHCs are linear (Figure 7). Employing these slopes has the added advantage of being independent of the summer concentrations, eliminating any effects of local camp pollution or periods below detection limit.

[48] The ratios of the slopes versus ethane are  $1.00$ ,  $0.59 \pm 0.1$ ,  $0.33 \pm 0.05$ ,  $0.26 \pm 0.08$ , and  $0.14 \pm 0.04$  for ethane, propane, ethyne, *n*-butane, and *i*-butane, respectively. The uncertainty is estimated as the standard deviation of the monthly slopes weighted by the sample number (Figure 7). For ease of comparison, we will present mixing ratios or emission estimates (weight estimates converted to molecular estimates) as ratios normalized to ethane as a percentage (ethane/ethane = 1 = 100%) for the remainder of this manuscript. Thus the above ratios are 100:59(±10):33(±5):26(±8):14(±4) for ethane, propane, ethyne, *n*-butane, and *i*-butane, respectively (Table 3). Pearson’s least squares correlation coefficients for the linear fits versus ethane are  $r^2 = 0.99$ , 0.96, 0.96, and 0.96 for propane, ethyne, *n*-butane, and *i*-butane, respectively. By comparison, the correlations versus ethane over the annual cycle are weaker with  $r^2$  values of 0.86, 0.92, 0.75, and 0.72 for propane, ethyne, *n*-butane, and *i*-butane, respectively (Figures 7b–7e). The correlation of the annual cycles in the above figures highlight the differences in photochemical lifetime between NMHCs and clearly reflect changes in the seasonal trend from the linear accumulation in the fall/winter, to rapid decay in the spring, and finally to slow decay or steady state in summer.

[49] Biogenic NMHC emissions are very important in remote vegetated terrestrial areas [Guenther *et al.*, 2000] as are concentrations of oxygenated species, whose abundance in remote regions is still largely unknown [Singh *et al.*,

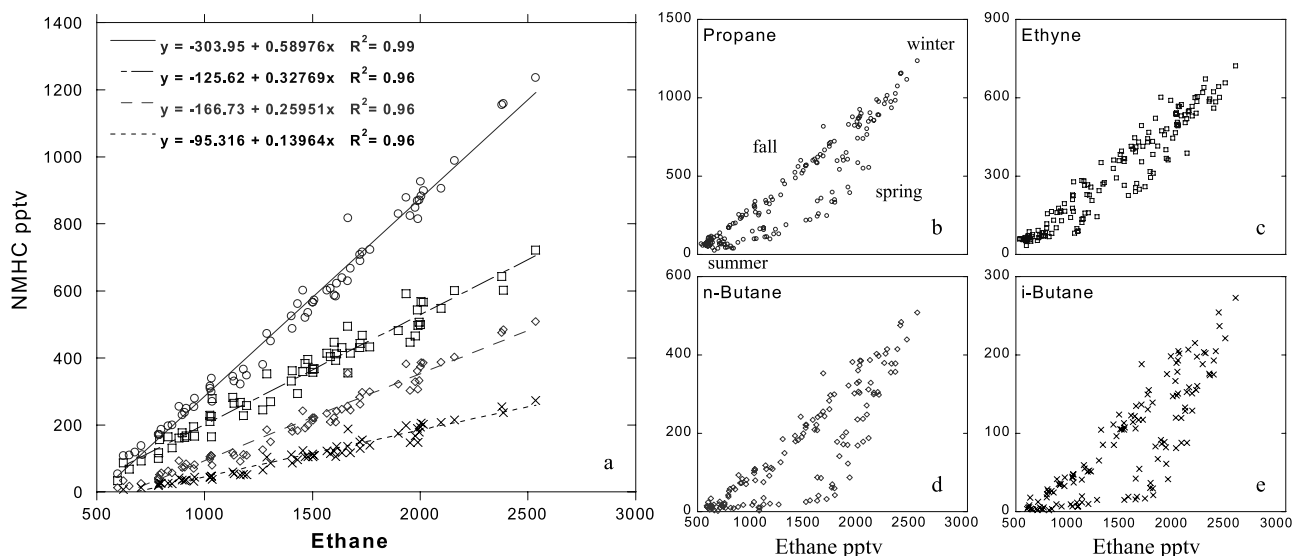


**Figure 7.** Linear correlation between ethane and other NMHCs for (a) fall increase (September 8–January 31) and entire year for (b) propane, (c) ethyne, (d) *n*-butane, and (e) *i*-butane. The seasons are indicated in the propane versus ethane plot in Figure 7b. The symbols are the same as in the smaller individual plots.



**Table 3.** Source Emission Ratios Normalized to Ethane (1 = 100) as a Percentage (in Molecules not Weight), and the Source Estimate for Global Emissions of Ethane in Tg ( $10^{12}$ ) Per Year

Source	Reference	Location	Tg yr <sup>-1</sup> Ethane	Ethane	Propane	Ethyne	<i>n</i> -Butane	<i>i</i> -Butane
Natural gas	<i>Blake et al.</i> [1992]	Alaska	NA	100	12	ND	5	NA
Oil production	<i>Blake et al.</i> [1992]	Prudhoe Bay, AK	NA	100	70	20	40	NA
Biomass burning	<i>Blake et al.</i> [1992]	Alaska	NA	100	8	38	<1	NA
Urban	<i>Blake et al.</i> [1992]	Anchorage, AK	NA	100	20	300	60	NA
Natural gas, crude	<i>Berger and Anderson</i> [1992]	oil pump, Oklahoma, USA	NA	100	71	ND	61	29
Biomass burning	<i>Andreae and Merlet</i> [2001] and M. O. Andreae (personal communication)	global estimate	7.6	100	20	81	2.5	0.9
Without biofuel			3.0	100	14	61	2.8	0.9
Urban/industrial	<i>Oliver et al.</i> [1996, 1999]	EDGAR 2.0					sum butanes	
Global			8.24	100	63	56	89	
>40°N			4.01	100	60	54	79	
Global	<i>Gupta et al.</i> [1998]	model	10.4	100	55	34	NA	NA
Summit ratios	this work	Summit, Greenland		100	59 ± 10	33 ± 5	26 ± 8	14 ± 4
Winter	<i>Goldstein et al.</i> [1995a]	Harvard Forest, MA		100	62	40	42	17
Summer	<i>Goldstein et al.</i> [1995a]	Harvard Forest, MA		100	70	56	44	21
PEM West A	<i>McKeen et al.</i> [1996]	Asian outflow		100	79	69	54	NA

2001]. However, we know from this work and the previous studies discussed earlier that ethane, propane, and ethyne are the most abundant anthropogenic NMHCs in the remote environment, and are present at high concentrations during winter throughout the NH. We suggest that the ratios we have calculated above represent averages for emissions to the mid- to high-latitude NH. Accurately simulating background NMHC mixing ratios are important for correct modeling of tropospheric chemistry [*Poisson et al.*, 2000; *Wang et al.*, 2001], so the ratios we have derived may be useful scalars for assessing how well global chemistry models simulate total emissions of these NMHCs.

[50] *Goldstein et al.* [1995a] employed a similar method to determine emission ratios versus ethyne for polluted air masses arriving at Harvard Forest over 2 months in summer and again for 2 months in winter. We have converted their results to emission ratios relative to ethane for comparison to Summit values (Table 3) [*Goldstein et al.*, 1995a]. The winter Harvard Forest emission ratios compare quite well with the Summit values, with only slightly higher ethyne and about 60% higher *n*-butane ratios (Table 3). Lower Summit butane ratios are to be expected as the result of loss of the short-lived species during the relatively long transit times to Summit. Thus the abundance of the shorter-lived NMHCs (i.e., the butanes) versus ethane for Summit should be considered to represent lower limits.

#### 4.3.1. Comparison of Emission Ratios With Source Emission Factors

[51] In Table 3, we compare the average ratios derived from our Summit observations with individual source signatures. This is a difficult task because individual source samples are subject to high spatial and temporal variability. This limitation also applies to the source emission factors derived for use in urban emission inventories which constrain air quality models [*Mollmann-Coers et al.*, 2002]. In a critical review, *Russell and Dennis* [2000] stated that emission estimate uncertainties appear to be the dominant limitation on the current ability of photochemical models to simulate urban and regional scale chemistry.

[52] Emission inventories typically are very complex, dealing with hundreds of compounds emitted by numerous, often independent, processes, including combustion and solvent evaporation as well as biogenic sources. Most

NMHC emission inventories are tailored to predict the air quality of urban airsheds.

[53] Global emission inventories, for example, the EDGAR [*Olivier et al.*, 1996, 1999], rely heavily upon these urban inventories. The simplifications and assumptions that have to be made to extrapolate these inventories spatially and temporally can cause problems, especially when the original emission factors themselves are subject to large uncertainties. For example, background levels of ethyne are often overestimated as the result of extrapolating combustion-dominated emissions from urban/industrial areas [*Blake et al.*, 1992; *Parrish et al.*, 1992; *Penkett et al.*, 1993]. By contrast, contributions from propane and butanes resulting from the evaporation of solvents and fuel, including liquid petroleum gas (LPG) leakage in urban areas such as Mexico City, are often underestimated [*Blake and Rowland*, 1995].

[54] The comparison between common light NMHC source signatures in Table 3 includes data from *Blake et al.* [1992] obtained during the summer 1988 Arctic Boundary Layer Expedition (ABLE 3A). The emission ratios display a wide range, representing the source categories urban emissions, biomass burning, natural gas and oil production losses. Remote mixing ratios of the NMHCs, such as measured at Summit, will then reflect a mixture of these sources.

#### 4.3.2. Impact of Sources on Background Ratios

[55] Returning to the plot of  $\ln(n\text{-butane/ethane})$  against  $\ln(\text{propane/ethane})$  (slope 1.58,  $r^2 = 0.91$ ) in Figure 4a, we recall that these data were indistinguishable from the slope of  $1.51 \pm 0.10$  derived from a large data set including near-source, rural continental, remote Pacific, and free tropospheric samples combined by *Parrish et al.* [1992]. Both slopes fall significantly below the calculated kinetic slope of approximately  $2.8 \pm 0.2$  expected from OH removal, which has been attributed mainly to the consequence of dilution [*Parrish et al.*, 1992; *McKeen and Liu*, 1993]. From this, *Parrish et al.* concluded that good agreement between air masses of vastly differing ages indicated that levels of light alkanes in all regions are dominated by anthropogenic sources characterized by relatively constant emission ratios.

[56] The fact that the slope derived from the Summit data is also similar supports the conclusions of *Parrish et al.* [1992], but the emission ratios listed in Table 3 are far from

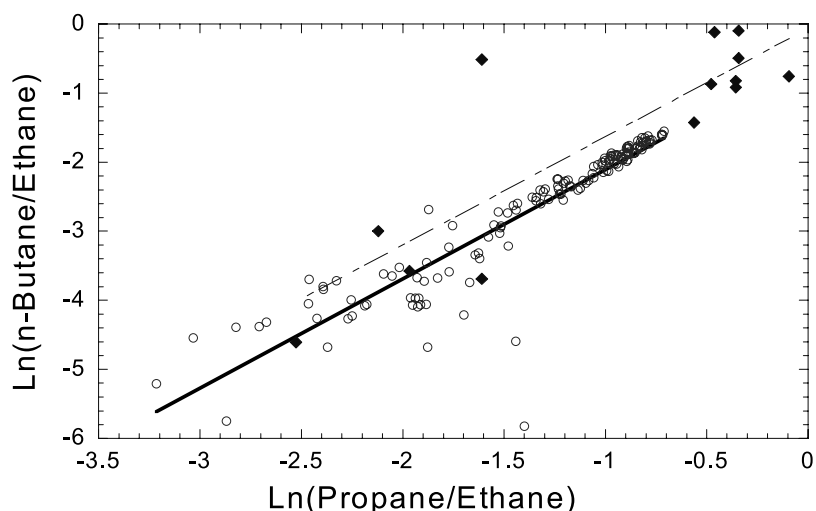


**Figure 8.** Plot of seasonal Summit data with source emission ratios overlaid for  $\text{Ln}(n\text{-butane/ethane})$  to  $\text{Ln}(\text{propane/ethane})$ . Urban and oil production lie to the upper right, while natural gas leakage and biomass burning lie to the lower left.

constant. If we overlay these source emission ratios on the plot of  $\text{Ln}(n\text{-butane/ethane})$  versus  $\text{Ln}(\text{propane/ethane})$  (Figure 8), we observe that urban emissions lie in the upper right corner along with gas venting/leakage from oil production and peak winter Summit concentrations, while biomass burning and natural gas emissions lie in the lower left corner with minimum summer Summit concentrations. The slope generated by these emission factors alone is 1.57 ( $r^2 = 0.73$ ), which is remarkably similar to the values derived from the Summit data set and by Parrish *et al.* [1992]. While this agreement may be purely coincidental, we argue that rather than relying on dilution alone, the influence of air masses with different source signatures may help to explain the observed deviation from the kinetic slope. Fresh urban air masses heavily influenced by butane emissions will tend to be diluted by air masses carrying a relatively remote signature with lower butane versus ethane ratios characteristic of biomass burning influence.

#### 4.3.3. The Special Influence of Nonurban Sources

[57] The composition of the winter NH troposphere is dominated by a mix of anthropogenic source emissions. However, farther away from urban source regions, aged background air will be more strongly influenced by any typically nonurban source, such as biomass burning, which is the dominant source of ethane and ethyne outside of urban areas [Rudolph, 1995]. Natural gas emissions from gas and oil extraction, as well as from gas hydrates, “natural” gas leakage, and coal mining, exists primarily outside of urban areas, so background air would also be biased by the ratios typical of these sources.

[58] For example, as we saw earlier, average alkane mixing ratios in December at Barrow are statistically elevated compared with the ratios at Summit (Figure 3). Enhancements are 509, 374, 184, and 87 pptv (ratios 100:73:36:17) for ethane, propane, *n*-butane, and *i*-butane, respectively, with no enhancement in ethyne. These enhancement ratios are very similar to those from oil production at Prudhoe Bay (Table 3). The Barrow propane/ethane ratio of 73 is also consistent with a corresponding value of 67 for fossil fuel usage [Rudolph, 1995] indicating

the influence of oil production rather than natural gas. In support of this distinction, Table 3 shows that the propane and butane emissions relative to ethane from an oil wellhead sampled in Oklahoma are much higher than a natural gas sample collected in Alaska. The town of Barrow (which is 8 km to the south of the sampling station) uses natural gas. However, the evidence presented above suggests that in December, the sampling site may be more influenced by the rich oil fields of the North Slope and oil drilling at Prudhoe Bay, rather than natural gas fuel emissions from the town. Learning more about the cause of the December enhancements compared to Summit would require higher resolution data from Barrow.

[59] As shown in Table 3, biomass burning emissions manifest a wide range of emission ratios, primarily depending on the type of fuel and whether the fires are predominantly smoldering or flaming [Lobert *et al.*, 1991]. A current review by Andreae and Merlet [2001], which includes biomass burning as well as charcoal and biofuel burning, gives emission ratios that include significant amounts of ethyne, propane, and butanes (Table 3). Inclusion of biofuels increases the contributions of propane and ethyne by about 70 and 30%, respectively (Table 3). The emission estimates for Alaskan biomass burning reveal relatively low contributions for gases other than ethane and ethyne, probably because the fire plumes were very well aged by the time they were sampled [Blake *et al.*, 1992].

#### 4.3.4. Comparison to Global Emission Estimates

[60] The EDGAR 2.0 total yearly emissions inventory for all high-latitude ( $>40^\circ\text{N}$ ) NH sources, including estimates of all fossil fuel usage, biofuel combustion (but not biomass burning), industrial process/solvent use, land use/waste treatment, and natural sources [Olivier *et al.*, 1996], are compared to the Summit ratios in Table 3. As predicted, the Summit butane values are somewhat low, as the result of dilution and photochemical aging, but the values for propane and ethyne are remarkably similar to the Summit ratios. However, the inclusion of biomass burning presumably would raise the EDGAR ratio for ethyne/ethane, while reducing the contributions of propane and the

butanes. If we include the estimates from biomass burning, without biofuel, scaled off the emission factors of *Andreae and Merlet* [2001] of 3.0, 0.64, 1.6, and 0.21 combined with EDGAR 2.0, then the total global source estimates are 11.2, 8.3, 5.6, and 14.3 Tg yr<sup>-1</sup> for ethane, propane, ethyne, and the butanes, respectively. The global molecular emission ratios are then 100:51:58:66 for ethane, propane, ethyne, and the butanes, which when compared to Summit is slightly low for propane, significantly elevated for ethyne, and still slightly elevated for the butanes. These are global emission estimates and temporal averages at that, so they are not necessarily good comparisons, but the general agreement indicates that the background ratios measured at Summit are representative of high NH emission ratios. The global estimates of *Gupta et al.* [1998], which are modeled global source strengths calculated from latitudinal distributions, are also very similar to, and even within one standard deviation of the Summit ratios for ethane, propane, and ethyne.

[61] A comparison of the Summit seasonal variations with preliminary model predictions from the NCAR Mozart global chemical transport model shows remarkable similarity for ethane, propane, and the butanes (which are lumped hydrocarbons of C<sub>4</sub> and greater) with just slightly lower winter concentrations (by about 10–20%) (X. Tie, personal communication). The Mozart model uses the EDGAR emission inventory with the addition of a separate inventory for biomass burning, ocean, and biogenic emissions. Preliminary model runs give confidence that current global emissions inventories are relatively precise. However, recent GEOS-CHEM global 3D model results for propane and butane distributions at Harvard Forest using the EDGAR inventory suggest that this inventory is too heavily weighted to emissions in the Middle East [*Jacob et al.*, 2002]. The fact that the background concentrations at Harvard Forest and Summit agree quite well, supports the conclusions of *Jacob et al.* [2002] that the version of the EDGAR inventory employed by GEOS-CHEM is flawed. The problem may simply be with the distribution of emissions in the EDGAR 2.0 inventory because its use in Mozart does not significantly bias simulation of the Summit seasonal trends. This simple comparison merely illustrates that the background Summit ratios represent an excellent test for modeled global source distributions.

#### 4.4. Alkyl Nitrates

##### 4.4.1. Seasonal Distributions

[62] The seasonal trend in total light C<sub>1</sub>–C<sub>4</sub> alkyl nitrates at Summit shows a broad peak through late winter from mid-January to April (Figure 2f) with total mixing ratios between 30 and 42 pptv dominated by 2-C<sub>3</sub>H<sub>7</sub>ONO<sub>2</sub> and 2-C<sub>4</sub>H<sub>9</sub>ONO<sub>2</sub>. The 2-C<sub>3</sub>H<sub>7</sub>ONO<sub>2</sub> and 2-C<sub>4</sub>H<sub>9</sub>ONO<sub>2</sub> mixing ratios comprise roughly 60% of the total alkyl nitrates through the winter. The winter dominance of C<sub>3</sub>–C<sub>4</sub> alkyl nitrates compares well with previously published data, but at slightly lower mixing ratios. During the 1992 Alert campaign (PSE92) in northern Canada, *Muthuramu et al.* [1994] measured nearly 35 pptv of C<sub>3</sub> and C<sub>4</sub> alkyl nitrates during peak winter concentrations, totaling roughly 50% of the light organic nitrate contribution.

[63] The alkyl nitrates also exhibit a trend in the timing of their winter maximum concentrations, where the alkyl

nitrates peak later in the winter with decreasing photochemical lifetime, first CH<sub>3</sub>ONO<sub>2</sub> and last 2-C<sub>4</sub>H<sub>9</sub>ONO<sub>2</sub> (Table 1). The trend in timing since winter solstice (December 21) of the peak values for the alkyl nitrates is the opposite to that seen for the NMHCs where the time from winter solstice to the peak value increases with increasing photochemical lifetime, i.e., ethane peaks latest. However, the summer minimum values show the same trend as the NMHCs, where the shortest lived species reach their minima earlier in the summer (Table 1). Since the longer chain alkyl nitrates are secondary species, it follows that 2-C<sub>3</sub>H<sub>7</sub>ONO<sub>2</sub> and 2-C<sub>4</sub>H<sub>9</sub>ONO<sub>2</sub> would peak after their respective parent hydrocarbons, but then would decay at a faster rate than methyl and ethyl nitrate as the result of their shorter photochemical lifetimes.

[64] We do not have any measurement of NO<sub>y</sub> during this seasonal study at Summit, but we can compare mixing ratios with previously published data to infer a NO<sub>y</sub> contribution. During the summers of 1998 and 1999 at Summit, measurements collected as part of the NSF-funded “Air-Snow Exchange of Reactive Nitrogen Oxides” project characterizing the boundary layer NO<sub>y</sub> budget indicated that approximately 8% of NO<sub>y</sub> was in the form of alkyl nitrates [R. Honrath, unpublished data, 1999; *Dibb et al.*, 1998]. Because summer concentrations of RONO<sub>2</sub> are only one third of the winter values, it is possible that the C<sub>1</sub>–C<sub>4</sub> alkyl nitrates at Summit contribute a similar amount (8%) of total NO<sub>y</sub> throughout the year, but joint measurements of NO<sub>y</sub> and alkyl nitrates would need to be made to show this. *Munger et al.* [1999] measured median spring-summer NO<sub>y</sub> values at Summit of 985 to 444 pptv from May to July, 1995, but the summer values of 1998 and 1999 were much lower at approximately 100 pptv total NO<sub>y</sub> (R. Honrath, unpublished data, 1999). The 1995 measurements by *Munger et al.* [1999] could be an anomalous year, but they at least indicate that there is no concise summertime concentration range of NO<sub>y</sub> at Summit. At Alert, Canada in 1988, *Bottenheim et al.* [1993] found that light alkyl nitrates contributed about 20% to the total NO<sub>y</sub>, while *Muthuramu et al.* [1994] measured a contribution between 7 and 20% NO<sub>y</sub> during the 1992 Alert campaign (PSE92) from 22 January to 22 April, with peak RONO<sub>2</sub> contribution near the end of February, similar to the peak in total alkyl nitrates at Summit. The Alert C<sub>1</sub>–C<sub>4</sub> alkyl nitrate mixing ratios measured by *Muthuramu et al.* [1994] are higher than Summit by about 10 pptv, but within the same winter range 25–45 pptv, thus it is likely that Summit contribution of RONO<sub>2</sub> to NO<sub>y</sub> is similar to that at Alert. During PSE92, 50% of the winter peak concentrations of alkyl nitrates were contributed by C<sub>5</sub>, C<sub>6</sub>, and larger unknown alkyl nitrates [*Muthuramu et al.*, 1994], which may also contribute to the total alkyl nitrates at Summit. Current field measurements by our group are attempting to determine the fraction of higher chain nitrates (C<sub>5</sub>–C<sub>6</sub>) to the total alkyl nitrates over a seasonal period at Summit.

##### 4.4.2. Sources

[65] Because alkyl nitrates are both primary oceanic and secondary products of emission from photochemical oxidation of HC in the presence of NO<sub>x</sub>, there are distinct differences between oceanic and urban emissions [*Blake et al.*, 1999, 2003b]. This makes them useful indicators of air mass origin and age. Measurements from areas of high

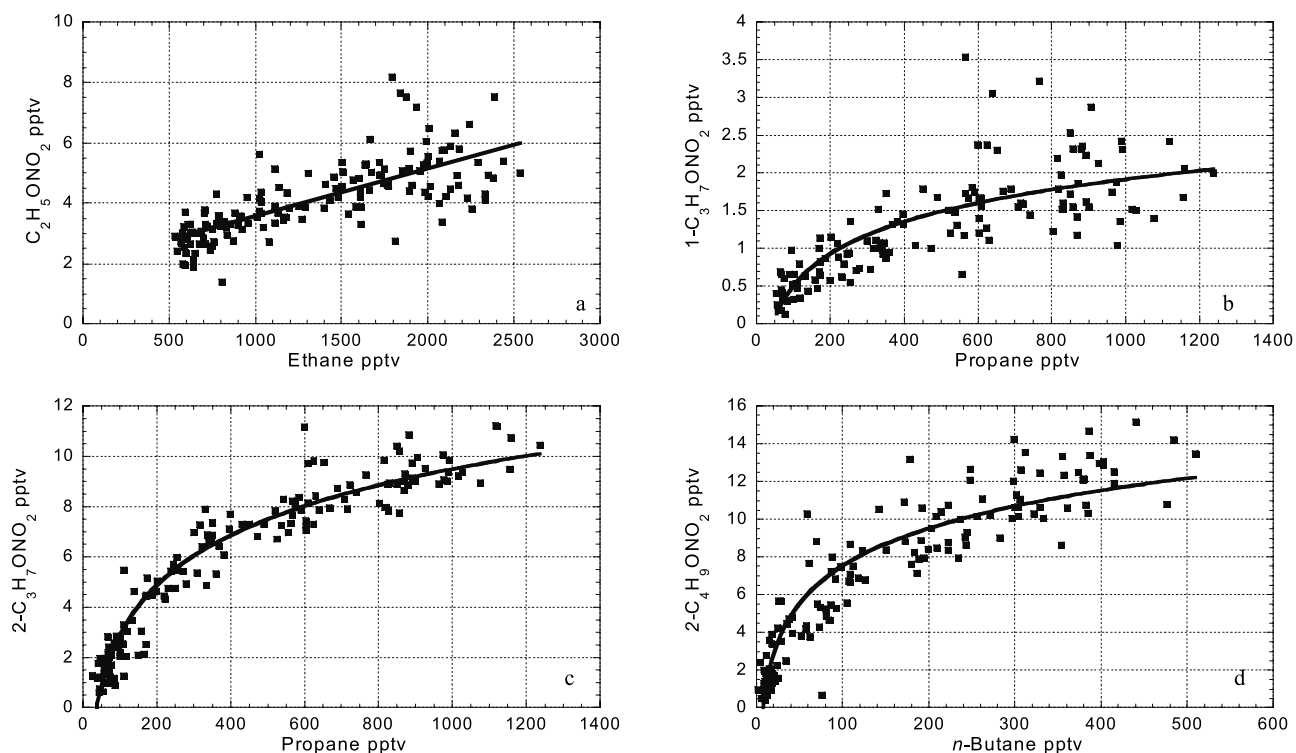


Figure 9. (a–d) Alkyl nitrates correlations to parent alkanes.

oceanic emissions, such as the equatorial Pacific, exhibit high methyl nitrate mixing ratios and show no significant emission of 2-butyl nitrate (50:1 for  $C_3H_5ONO_2$ : $2-C_4H_9ONO_2$ ) [Atlas *et al.*, 1997; Blake *et al.*, 2003b]. By contrast, gas-phase photochemical production of alkyl nitrates is heavily weighted to the longer-chain species because their yield increases rapidly with chain length [Atkinson *et al.*, 1982; Roberts, 1990; Arey *et al.*, 2001]. This production is balanced by fast photochemical loss of the longer-chain alkyl nitrates, so that 2-butyl nitrate typically is the dominant alkyl nitrate in fairly fresh urban pollution plumes, while methyl and ethyl are dominant in very aged air masses.

[66] Sea salt ions reach Summit principally in winter and spring [Whitlow *et al.*, 1992], consistent with the observation that methyl nitrate peaks in winter (but at much lower enhancements than for the heavier alkyl nitrates). Oceanic emissions of  $C_1$ – $C_2$  alkyl nitrates are characterized by a methyl/ethyl nitrate emission ratio of approximately three [Blake *et al.*, 1999, 2003a]. Photochemical aging would only increase this ratio in favor of longer-lived methyl nitrate. Thus the low levels of methyl nitrate and the near one-to-one correlation with ethyl nitrate (Figures 2a and 2b) indicate that high-latitude NH waters are not a large source of  $C_1$ – $C_2$  alkyl nitrates.

[67] The correlations between the alkyl nitrates and parent alkanes for  $C_2$ – $C_4$  (Figures 9a–9d) are strongest for 2-propyl and 2-butyl nitrate versus propane and *n*-butane, respectively. These relationships are nonlinear as the result of the fact that, while rates of oxidation of the alkanes to produce the alkyl nitrates decreases into the winter, emissions of the alkanes remain relatively constant. Some of this nonlinearity may also reflect periods when HC oxidation can occur, but levels of  $NO_x$  are too low for alkyl

nitrates to be produced, e.g., in the vicinity of fuel leakage from oil and natural gas drilling. By contrast, the corresponding correlation for ethyl nitrate versus ethane, reveals a higher degree of variability and produces a linear correlation ( $r^2$  values of 0.56). The linear nature of the ethyl nitrate versus ethane curve is likely caused by the high background concentration of ethane, which never approaches zero, whereas the shorter-lived alkanes exhibit a logarithmic decay as they approach zero.

## 5. Summary

[68] The full seasonal cycles presented for  $C_2$ – $C_4$  NMHCs and  $C_1$ – $C_4$  alkyl nitrates at Summit, Greenland, display a clear late winter maximum and a broad summer minimum for each gas. Their levels reflect a sampling site far removed from local and regional sources, but influenced by long-range transport and photochemical removal. Comparison with the literature confirms that year-to-year seasonal NMHC oscillations are very reproducible, with the relatively low mixing ratios measured at Summit marking it as the most remote site used in the comparison. However, close similarities with measurements at the sea level site in Barrow indicate that even though Summit is located at 3 km, it should be thought of as a lower tropospheric (0–3 km) site more influenced by planetary boundary layer air than by the free troposphere.

[69] In autumn, when the NMHCs exhibit a linear increase with time as NH emissions start to build up at high latitudes, the NMHCs are highly correlated with each other. We compared the ratios of their slopes relative to ethane to emission factors versus ethane for a wide variety of sources, revealing a great deal of variability. However, the Summit ratios were much closer to those obtained from



model estimates of high-latitude NH and global emission averages. We suggest that these Summit ratios represent a useful average of combined NH sources, so provide an important test of the performance of the current emission inventories employed in global chemistry models.

[70] We presented complete annual cycles for the suite of C<sub>1</sub>–C<sub>4</sub> alkyl nitrates, which provide further insight into the influence of oceanic and aged urban air masses on the remote Arctic troposphere. Comparison of the seasonal trends of the alkyl nitrates with their parent NMHCs is complicated, but these data will be invaluable to the global modeling community in validating emissions, photochemistry, and transport in 3D models.

[71] **Acknowledgments.** We would like to acknowledge the heroic contribution of science technicians Bob Hawley and Sarah Sturges, who collected the samples throughout the cold dark days of winter isolated on the ice sheet with Pat Smith and Phil Austin. We would also like to thank Murray McEachern, Brent Love, John Bilicska, and the other helpful technicians at the UCI laboratory, plus Isobel Simpson and Jack Dibb for manuscript comments. This research received funding from NSF OPP.

## References

- Andreae, M. O., and P. Merlet, Emission of trace gases and aerosols from biomass burning, *Global Biogeochem. Cycles*, 15(4), 955–966, 2001.
- Apel, E. C., J. G. Calvert, and F. C. Fehsenfeld, The nonmethane hydrocarbon intercomparison experiment (Nomhice)—Task-1 and task-2, *J. Geophys. Res.*, 99(D8), 16,651–16,664, 1994.
- Arey, J., S. M. Aschmann, E. S. C. Kwok, and R. Atkinson, Alkyl nitrate, hydroxyalkyl nitrate, and hydroxycarbonyl formation from the NO<sub>x</sub>-air photooxidations of C-5–C-8 n-alkanes, *J. Phys. Chem. A*, 105(6), 1020–1027, 2001.
- Atkinson, R., Atmospheric chemistry of VOCs and NO<sub>x</sub>, *Atmos. Environ.*, 34, 2063–2101, 2000.
- Atkinson, R., S. M. Aschmann, W. P. L. Carter, A. M. Winer, and J. N. Pitts, Alkyl nitrate formation from the NO<sub>x</sub>-air photooxidations of C2–C8 n-alkanes, *J. Phys. Chem.*, 86(23), 4563–4569, 1982.
- Atkinson, R., D. L. Baulch, R. A. Cox, R. F. Hampson Jr., J. A. Kerr, M. J. Rossi, and J. Troe, Evaluated kinetic and photochemical data for atmospheric chemistry: Supplement VI. IUPAC subcommittee on gas kinetic data evaluation for atmospheric chemistry, *J. Phys. Chem. Ref. Data*, 26, 1329–1499, 1997.
- Atlas, E. L., and B. A. Ridley, The Mauna Loa Observatory photochemistry experiment: Introduction, *J. Geophys. Res.*, 101(D9), 14,531–14,541, 1996.
- Atlas, E., F. Flocke, S. Schauffler, V. Stroud, D. Blake, and F. S. Rowland, Evidence for marine sources of atmospheric alkyl nitrates: Measurements over the tropical Pacific Ocean during PEM-tropics, *Eos Trans. AGU*, 78(46), Fall Meet. Suppl., F115, 1997.
- Barrie, L. A., Arctic air pollution: An overview of current knowledge, *Atmos. Environ.*, 20, 643–663, 1986.
- Barrie, L. A., J. W. Bottenheim, and W. R. Hart, Polar sunrise experiment 1992 (Pse-1992)—Preface, *J. Geophys. Res.*, 99(D12), 25,313–25,314, 1994.
- Beine, H. J., D. A. Jaffe, D. R. Blake, E. Atlas, and J. Harris, Measurements of pan, alkyl nitrates, ozone, and hydrocarbons during spring in interior Alaska, *J. Geophys. Res.*, 101(D7), 12,613–12,619, 1996.
- Berger, B. D., and K. E. Anderson, *Modern Petroleum: A Basic Primer of the Industry*, xvi, 517 pp., PennWell Books, Tulsa, Okla., 1992.
- Bertman, S. B., J. M. Roberts, D. D. Parrish, M. P. Buhr, P. D. Goldan, W. C. Kuster, F. C. Fehsenfeld, S. A. Montzka, and H. Westberg, Evolution of alkyl nitrates with air mass age, *J. Geophys. Res.*, 100(D11), 22,805–22,813, 1995.
- Blake, D. R., and F. S. Rowland, Global atmospheric concentration and source strength of ethane, *Nature*, 321, 231–233, 1986.
- Blake, D. R., and F. S. Rowland, Urban leakage of liquefied petroleum gas and its impact on Mexico City air quality, *Science*, 269(5226), 953–956, 1995.
- Blake, D. R., D. F. Hurst, T. W. Smith, W. J. Whipple, T. Y. Chen, N. J. Blake, and F. S. Rowland, Summertime measurements of selected nonmethane hydrocarbons in the arctic and subarctic during the 1988 Arctic boundary layer expedition (Able-3a), *J. Geophys. Res.*, 97(D15), 16,559–16,588, 1992.
- Blake, N. J., D. R. Blake, B. C. Sive, T. Y. Chen, F. S. Rowland, J. E. Collins, G. W. Sachse, and B. E. Anderson, Biomass burning emissions and vertical distribution of atmospheric methyl halides and other reduced carbon gases in the South Atlantic Region, *J. Geophys. Res.*, 101(D19), 24,151–24,164, 1996.
- Blake, N. J., et al., Aircraft measurements of the latitudinal, vertical, and seasonal variations of NMHCs, methyl nitrate, methyl halides, and DMS during the first aerosol characterization experiment (ACE 1), *J. Geophys. Res.*, 104(D17), 21,803–21,817, 1999.
- Blake, N. J., D. R. Blake, B. C. Sive, A. S. Katzenstein, S. Meinardi, O. W. Wingenter, B. A. Ridley, and F. S. Rowland, The seasonal evolution of NMHCs, and light alkyl nitrates at mid to high northern latitudes during TOPSE, *J. Geophys. Res.*, 108, doi:10.1029/2001JD001467, in press, 2003a.
- Blake, N. J., A. L. Swanson, D. R. Blake, E. Atlas, F. Flocke, and F. S. Rowland, Latitudinal, vertical, and seasonal variations of C1–C4 alkyl nitrates in the troposphere over the Pacific Ocean during PEM-tropics A and B: Oceanic and continental sources, *J. Geophys. Res.*, 108, doi:10.1029/2001JD001444, in press, 2003b.
- Bodhaine, B. A., and E. G. Dutton, A long term decrease in Arctic Haze at Barrow, Alaska—Reply, *Geophys. Res. Lett.*, 22(6), 741–742, 1995.
- Bodhaine, B. A., E. G. Dutton, and J. J. DeLuise, Surface aerosol measurements at Barrow during AGASP, *Geophys. Res. Lett.*, 11, 377–380, 1984.
- Bottenheim, J. W., and M. F. Shepherd, C2–C6 hydrocarbon measurements at 4 rural locations across Canada, *Atmos. Environ.*, 29, 647–664, 1995.
- Bottenheim, J. W., L. A. Barrie, and E. Atlas, The partitioning of nitrogen oxides in the lower Arctic troposphere during spring 1988, *J. Atmos. Chem.*, 17(1), 15–27, 1993.
- Boudries, H., G. Toupance, and A. L. Dutot, Seasonal-variation of atmospheric nonmethane hydrocarbons on the western coast of Brittany, France, *Atmos. Environ.*, 28, 1095–1112, 1994.
- Cassano, J. J., J. E. Box, D. H. Bromwich, L. Li, and K. Steffen, Evaluation of polar MM5 simulations of Greenland's atmospheric circulation, *J. Geophys. Res.*, 106(D24), 33,867–33,889, 2001.
- Chen, T.-Y., Three-dimensional distribution of nonmethane hydrocarbons and halocarbons over the northwestern Pacific and the temporal and spatial variations of oceanic methyl iodide emissions, Ph.D. dissertation, Univ. of Calif., Irvine, 1996.
- Clemmishaw, K. C., J. Williams, O. V. Rattigan, D. E. Shallcross, K. S. Law, and R. A. Cox, Gas-phase ultraviolet absorption cross-sections and atmospheric lifetimes of several C-2–C-5 alkyl nitrates, *J. Photochem. Photobiol. A*, 102(2–3), 117–126, 1997.
- Colman, J. J., A. L. Swanson, S. Meinardi, B. C. Sive, D. R. Blake, and F. S. Rowland, Description of the analysis of a wide range of volatile organic compounds in whole air samples collected during PEM-tropics A and B, *Anal. Chem.*, 73(15), 3723–3731, 2001.
- Dibb, J. E., M. Arsenault, R. Honrath, M. Peterson, S. Guo, P. Shepson, B. Campbell, N. J. Blake, D. R. Blake, and S. Bertman, Reactive nitrogen oxides at Summit, Greenland, *Eos Trans. AGU*, 79(45), Fall Meet. Suppl., F95, 1998.
- Ehhalt, D. H., U. Schmidt, R. Zander, P. Demoulin, and C. P. Rinsland, Seasonal cycle and secular trend of the total and tropospheric column abundance of ethane above the Jungfraujoch, *J. Geophys. Res.*, 96(D3), 4985–4994, 1991.
- Finlayson-Pitts, B. J., Indications of photochemical histories of Pacific air masses from measurements of atmospheric trace species at Point-Arena, California: Comment, *J. Geophys. Res.*, 98(D8), 14,991–14,993, 1993.
- Finlayson-Pitts, B. J., and J. N. Pitts, *Chemistry of the Upper and Lower Atmosphere: Theory, Experiments, and Applications*, vol. xxii, p. 969, Academic, San Diego, Calif., 2000.
- Flocke, F., A. VolzThomas, H. J. Buers, W. Patz, H. J. Garthe, and D. Kley, Long-term measurements of alkyl nitrates in southern Germany, 1, General behavior and seasonal and diurnal variation, *J. Geophys. Res.*, 103(D5), 5729–5746, 1998.
- Friedrich, R., and A. Obermeier, Anthropogenic emissions of volatile organic compounds, in *Reactive Hydrocarbons in the Atmosphere*, edited by C. N. Hewitt, pp. 2–38, Academic, San Diego, Calif., 1999.
- Goldstein, A. H., S. C. Wofsy, and C. M. Spivakovsky, Seasonal variations of nonmethane hydrocarbons in rural New England—Constraints on OH concentrations in northern midlatitudes, *J. Geophys. Res.*, 100(D10), 21,023–21,033, 1995a.
- Goldstein, A. H., B. C. Daube, J. W. Munger, and S. C. Wofsy, Automated in-situ monitoring of atmospheric nonmethane hydrocarbon concentrations and gradients, *J. Atmos. Chem.*, 21(1), 43–59, 1995b.
- Greenberg, J. P., D. Helmig, and P. R. Zimmerman, Seasonal measurements of nonmethane hydrocarbons and carbon monoxide at the Mauna Loa Observatory during the Mauna Loa Observatory photochemistry experiment, 2, *J. Geophys. Res.*, 101(D9), 14,581–14,598, 1996.
- Guenther, A., C. Geron, T. Pierce, B. Lamb, P. Harley, and R. Fall, Natural emissions of non-methane volatile organic compounds; carbon monox-

- ide, and oxides of nitrogen from North America, *Atmos. Environ.*, **34**, 2205–2230, 2000.
- Gupta, M. L., R. J. Cicerone, D. R. Blake, F. S. Rowland, and I. S. A. Isaksen, Global atmospheric distributions and source strengths of light hydrocarbons and tetrachloroethene, *J. Geophys. Res.*, **103**(D21), 28,219–28,235, 1998.
- Hagerman, L. M., V. P. Aneja, and W. A. Lonneman, Characterization of non-methane hydrocarbons in the rural southeast United States, *Atmos. Environ.*, **31**, 4017–4038, 1997.
- Haggen-Smit, A. J., Chemistry and physiology of Los Angeles smog, *Ind. Eng. Chem.*, **44**, 1342–1346, 1952.
- Honrath, R. E., and D. A. Jaffe, The seasonal cycle of nitrogen-oxides in the Arctic troposphere at Barrow, Alaska, *J. Geophys. Res.*, **97**(D18), 20,615–20,630, 1992.
- Hov, O., S. A. Penkett, I. S. A. Isaksen, and A. Semb, Organic gases in the Norwegian Sea, *Geophys. Res. Lett.*, **11**, 425–428, 1984.
- Hov, O., N. Schmidbauer, and M. Oehme, Light hydrocarbons in the Norwegian Arctic, *Atmos. Environ.*, **23**, 2471–2482, 1989.
- Hurst, D. F., Seasonal variations in the latitudinal distribution of tropospheric carbon monoxide, 1986–1988, Ph.D. dissertation, Univ. of Calif., Irvine, 1990.
- Jacob, D. J., B. D. Field, E. M. Jin, I. Bey, Q. Li, J. A. Logan, R. M. Yantosca, and H. B. Singh, Atmospheric budget of acetone, *J. Geophys. Res.*, **107**(D10), 4100, doi:10.1029/2001JD000694, 2002.
- Jobson, B. T., Z. Wu, H. Niki, and L. A. Barrie, Seasonal trends of isoprene, C-2–C-5 alkanes, and acetylene at a remote boreal site in Canada, *J. Geophys. Res.*, **99**(D1), 1589–1599, 1994a.
- Jobson, B. T., H. Niki, Y. Yokouchi, J. Bottenheim, F. Hopper, and R. Leaitch, Measurements of C-2–C-6 hydrocarbons during the polar sunrise 1992 experiment: Evidence for Cl atom and Br atom chemistry, *J. Geophys. Res.*, **99**(D12), 25,355–25,368, 1994b.
- Kahl, J. D. W., D. A. Martinez, H. Kuhns, C. I. Davidson, J. L. Jaffrezo, and J. M. Harris, Air mass trajectories to Summit, Greenland: A 44-year climatology and some episodic events, *J. Geophys. Res.*, **102**(C12), 26,861–26,875, 1997.
- Kahl, J. D. W., J. A. Galbraith, and D. A. Martinez, Decadal-scale variability in long-range atmospheric transport to the Summit of the Greenland Ice Sheet, *Geophys. Res. Lett.*, **26**(4), 481–484, 1999.
- Kanakidou, M., H. B. Singh, K. M. Valentin, and P. J. Crutzen, A 2-dimensional study of ethane and propane oxidation in the troposphere, *J. Geophys. Res.*, **96**(D8), 15,395–15,413, 1991.
- Klonecki, A., et al., Seasonal changes in the transport of pollutants into the arctic troposphere-model study, *J. Geophys. Res.*, **108**, doi:10.1029/2002JD002199, in press, 2003.
- Laurila, T., and H. Hakola, Seasonal cycle of C-2–C-5 hydrocarbons over the Baltic Sea and northern Finland, *Atmos. Environ.*, **30**, 1597–1607, 1996.
- Lindskog, A., and J. Moldanova, The influence of the origin, season and time of the day on the distribution of individual NMHC measured at Rorvik, Sweden, *Atmos. Environ.*, **28**, 2383–2398, 1994.
- Lober, J. M., D. H. Scharffe, W.-M. Hao, T. A. Kuhlbusch, R. Seuwen, P. Warneck, and P. J. Crutzen, Experimental evaluation of biomass burning emissions: Nitrogen and carbon containing compounds, in *Global Biomass Burning—Atmospheric, Climatic, and Biospheric Implications*, edited by J. S. Levine, MIT Press, Cambridge, Mass., 1991.
- Lopez-Palma, J. D. P., Seasonality and global growth trends of carbon monoxide during 1995–2001, Univ. of Calif., Irvine, 2002.
- McKeen, S. A., and S. C. Liu, Hydrocarbon ratios and photochemical history of air masses, *Geophys. Res. Lett.*, **20**(21), 2363–2366, 1993.
- McKeen, S. A., S. C. Liu, E. Y. Hsie, X. Lin, J. D. Bradshaw, S. Smyth, G. L. Gregory, and D. R. Blake, Hydrocarbon ratios during Pem-West A—A model perspective, *J. Geophys. Res.*, **101**(D1), 2087–2109, 1996.
- Mollmann-Coers, M., D. Klemp, K. Mannschreck, and F. Slemr, Statistical study of the diurnal variation of modeled and measured NMHC contributions, *Atmos. Environ.*, **36**, S109–S122, 2002.
- Munger, J. W., D. J. Jacob, S. M. Fan, A. S. Colman, and J. E. Dibb, Concentrations and snow-atmosphere fluxes of reactive nitrogen at Summit, Greenland, *J. Geophys. Res.*, **104**(D11), 13,721–13,734, 1999.
- Muthuramu, K., P. B. Shepson, J. W. Bottenheim, B. T. Jobson, H. Niki, and K. G. Anlauf, Relationships between organic nitrates and surface ozone destruction during polar sunrise experiment 1992, *J. Geophys. Res.*, **99**(D12), 25,369–25,378, 1994.
- Nelson, P. F., and S. M. Quigley, Non-methane hydrocarbons in the atmosphere of Sydney, Australia, *Environ. Sci. Technol.*, **16**(10), 650–655, 1982.
- Olivier, J. G. J., A. F. Bouwman, C. W. M. Van der Maas, J. J. M. Berdowski, C. Veldt, J. P. J. Bloos, A. J. H. Visschedijk, P. Y. J. Zandveld, and J. L. Haverlag, Description of EDGAR version 2.0: A set of emission inventories of greenhouse gases and ozone depleting substances for all anthropogenic and most natural sources on a per country basis and on  $1^\circ \pm 1^\circ$  grid, in *RIVM Rep. 771060002*, Natl. Inst. of Public Health and the Environ., Bilthoven, Netherlands., 1996.
- Olivier, J. G. J., A. F. Bouwman, J. J. M. Berdowski, C. Veldt, J. P. J. Bloos, A. J. H. Visschedijk, C. W. M. van de Maas, and P. Y. J. Zandveld, Sectoral emission inventories of greenhouse gases for 1990 on a per country basis as well as on  $1^\circ \pm 1^\circ$ , *Environ. Sci. Policy*, **2**, 241–264, 1999.
- Parrish, D. D., C. J. Hahn, E. J. Williams, R. B. Norton, F. C. Fehsenfeld, H. B. Singh, J. D. Shetter, B. W. Gandrud, and B. A. Ridley, Indications of photochemical histories of Pacific air masses from measurements of atmospheric trace species at Point Arena, California, *J. Geophys. Res.*, **97**(D14), 15,883–15,901, 1992.
- Penkett, S. A., and K. A. Brice, The spring maximum in photo-oxidants in the Northern Hemisphere troposphere, *Nature*, **319**, 655–657, 1986.
- Penkett, S. A., N. J. Blake, P. Lightman, A. R. W. Marsh, P. Anwyl, and G. Butcher, The seasonal variation of nonmethane hydrocarbons in the free troposphere over the North Atlantic Ocean—Possible evidence for extensive reaction of hydrocarbons with the nitrate radical, *J. Geophys. Res.*, **98**(D2), 2865–2885, 1993.
- Poisson, N., M. Kanakidou, and P. J. Crutzen, Impact of non-methane hydrocarbons on tropospheric chemistry and the oxidizing power of the global troposphere: 3-Dimensional modelling results, *J. Atmos. Chem.*, **36**(2), 157–230, 2000.
- Ridley, B. A., M. A. Carroll, and G. L. Gregory, Measurements of nitric oxide in the boundary layer and free troposphere over the Pacific Ocean, *J. Geophys. Res.*, **92**(D2), 2025–2047, 1987.
- Ridley, B. A., et al., Ozone depletion events observed in the high latitude surface layer during the TOPSE aircraft program, *J. Geophys. Res.*, **108**, doi:10.1029/2001JD001507, in press, 2003.
- Rinsland, C. P., et al., Northern and Southern hemisphere ground-based infrared spectroscopic measurements of tropospheric carbon monoxide and ethane, *J. Geophys. Res.*, **103**(D21), 28,197–28,217, 1998.
- Rinsland, C. P., E. Mahieu, R. Zander, P. Demoulin, J. Forrer, and B. Buchmann, Free tropospheric CO, C<sub>2</sub>H<sub>6</sub>, and HCN above central Europe: Recent measurements from the Jungfraujoch station including the detection of elevated columns during 1998, *J. Geophys. Res.*, **105**(D19), 24,235–24,249, 2000.
- Roberts, J. M., The atmospheric chemistry of organic nitrates, *Atmos. Environ.*, **24**, 243–287, 1990.
- Roberts, J. M., F. C. Fehsenfeld, S. C. Liu, M. J. Bollinger, C. Hahn, D. L. Albritton, and R. E. Sievers, Measurements of aromatic hydrocarbon ratios and NO<sub>x</sub> concentrations in the rural troposphere: Observation of air mass photochemical aging and NO<sub>x</sub> removal, *Atmos. Environ.*, **18**, 2421–2432, 1984.
- Roberts, J. M., R. S. Jutte, F. C. Fehsenfeld, D. L. Albritton, and R. E. Sievers, Measurements of anthropogenic hydrocarbon concentration ratios in the rural troposphere: Discrimination between background and urban sources, *Atmos. Environ.*, **19**, 1945–1950, 1985.
- Rudolph, J., The tropospheric distribution and budget of ethane, *J. Geophys. Res.*, **100**(D6), 11,369–11,381, 1995.
- Rudolph, J., and F. J. Johnen, Measurements of light atmospheric hydrocarbons over the Atlantic in regions of low biological activity, *J. Geophys. Res.*, **95**(D12), 20,583–20,591, 1990.
- Rudolph, J., R. Koppmann, and C. Plass-Dulmer, The budgets of ethane and tetrachloroethene: Is there evidence for an impact of reactions with chlorine atoms in the troposphere?, *Atmos. Environ.*, **30**, 1887–1894, 1996.
- Russell, A., and R. Dennis, NARSTO critical review of photochemical models and modeling, *Atmos. Environ.*, **34**, 2283–2324, 2000.
- Schere, K. L., and G. M. Hidy, NARSTO critical reviews, *Atmos. Environ.*, **34**, 1853–1860, 2000.
- Scheuer, E., R. W. Talbot, J. E. Dibb, G. K. Seid, L. DeBell, and B. Lefer, Seasonal distribution of fine aerosol sulfate in the North American Arctic Basin during TOPSE, *J. Geophys. Res.*, **108**, doi:10.1029/2001JD001364, in press, 2003.
- Sharma, U. K., Y. Kajii, and H. Akimoto, Seasonal variation of C-2–C-6 NMHCs at Haplo, a remote site in Japan, *Atmos. Environ.*, **34**, 4447–4458, 2000.
- Singh, H. B., and P. B. Zimmerman, Atmospheric distribution and sources of nonmethane hydrocarbons, in *Gaseous Pollutants: Characterization and Cycling*, edited by J. O. Nriagu, John Wiley, New York, 1992.
- Singh, H., Y. Chen, A. Staudt, D. Jacob, D. Blake, B. Heikes, and J. Snow, Evidence from the Pacific troposphere for large global sources of oxygenated organic compounds, *Nature*, **410**(6832), 1078–1081, 2001.
- Sive, B. C., Atmospheric nonmethane hydrocarbons: Analytical methods and estimated hydroxyl radical concentrations, Ph.D. dissertation, Univ. of Calif., Irvine, 1998.
- Smyth, S. B., et al., Factors influencing the upper free tropospheric distribution of reactive nitrogen over the South Atlantic during the trace a experiment, *J. Geophys. Res.*, **101**(D19), 24,165–24,186, 1996.

- Solberg, S., C. Dye, N. Schmidbauer, A. Herzog, and R. Gehrig, Carbonyls and nonmethane hydrocarbons at rural European sites from the Mediterranean to the Arctic, *J. Atmos. Chem.*, 25(1), 33–66, 1996.
- Spivakovsky, C. M., et al., Three-dimensional climatological distribution of tropospheric OH: Update and evaluation, *J. Geophys. Res.*, 105(D7), 8931–8980, 2000.
- Steffen, K., and J. Box, Surface climatology of the Greenland ice sheet: Greenland climate network 1995–1999, *J. Geophys. Res.*, 106(D24), 33,951–33,964, 2001.
- Talukdar, R. K., J. B. Burkholder, M. Hunter, M. K. Gilles, J. M. Roberts, and A. R. Ravishankara, Atmospheric fate of several alkyl nitrates, part 2, UV absorption cross-sections and photodissociation quantum yields, *J. Chem. Soc. Faraday Trans.*, 93(16), 2797–2805, 1997.
- Wang, K. Y., J. A. Pyle, D. E. Shallcross, and S. M. Hall, Formulation and evaluation of IMS, an interactive three-dimensional tropospheric chemical transport model, part 3, Comparison of modelled C-2–C-5 hydrocarbons with surface measurements, *J. Atmos. Chem.*, 40(2), 123–170, 2001.
- Whitlow, S., P. A. Mayewski, and J. E. Dibb, A comparison of major chemical species seasonal concentration and accumulation at the south pole and Summit, Greenland, *Atmos. Environ.*, 26, 2045–2054, 1992.
- Yienger, J. J., A. A. Klonecki, H. Levy, W. J. Moxim, and G. R. Carmichael, An evaluation of chemistry's role in the winter-spring ozone maximum found in the northern midlatitude free troposphere, *J. Geophys. Res.*, 104(D3), 3655–3667, 1999.

---

E. Atlas and F. Flocke, Atmospheric Chemistry Division, National Center for Atmospheric Research, 1850 Table Mesa Drive, Boulder, CO 80307, USA.

D. R. Blake, N. J. Blake, F. S. Rowland, and A. L. Swanson, Department of Chemistry, University of California at Irvine, 516 Rowland Hall, Irvine, CA 92697-2025, USA. (drblake@uci.edu; aswanson@ea.oac.uci.edu)